

1974

Surface elongation and interfacial sliding during gold-gold thermocompression bonding /

Ronald Paul Stapleton
Lehigh University

Follow this and additional works at: <https://preserve.lehigh.edu/etd>

 Part of the [Metallurgy Commons](#)

Recommended Citation

Stapleton, Ronald Paul, "Surface elongation and interfacial sliding during gold-gold thermocompression bonding /" (1974). *Theses and Dissertations*. 4463.
<https://preserve.lehigh.edu/etd/4463>

This Thesis is brought to you for free and open access by Lehigh Preserve. It has been accepted for inclusion in Theses and Dissertations by an authorized administrator of Lehigh Preserve. For more information, please contact preserve@lehigh.edu.

SURFACE ELONGATION AND INTERFACIAL SLIDING
DURING GOLD-GOLD THERMOCOMPRESSION BONDING

By

Ronald Paul Stapleton

A Thesis

Presented to the Graduate Committee

of Lehigh University

in Candidacy for the Degree of

Master of Science

in

Metallurgy and Materials Science

Lehigh University

1974

CERTIFICATE OF APPROVAL

This thesis is accepted and approved in partial fulfillment
of the requirements for the degree of Master of Science.

Date

Professor in Charge

Chairman of the Department
of Metallurgy and Materials Science

ACKNOWLEDGMENTS

The author wishes to make the following acknowledgments:

Dr. J. J. Svitak, Western Electric Co., ERC, for his technical assistance and inspiration throughout the course of this investigation.

Dr. W. C. Hahn, Jr., Lehigh University, for his support and guidance during the preparation of this manuscript. Mr. Leon Dries, Western Electric Co., Allentown Works, for his assistance and prior work which made this investigation possible.

Mr. Frank Paulus, Western Electric Co., ERC, for the scanning electron microscopy.

Mr. George Ziegenfuss, Western Electric Co., Allentown Works, for the emission spectrographic analysis.

The technical support staff of Dept. 02246, Western Electric Co., ERC, for their assistance and suggestions during the experimental work.

The Western Electric Company for providing the opportunity to attend this program.

TABLE OF CONTENTS

	<u>PAGE</u>
Abstract	1
I. Introduction	2
II. Experimental Procedure	6
III. Results and Discussion	12
A. Varying Substrate Plating Thickness	13
B. Surface Contamination	16
C. Symmetric Conditions	18
IV. Summary and Conclusions	21
Bibliography	48
Vita	50

LIST OF TABLES

	<u>PAGE</u>
Table I - Bond and Specimen Parameters.	25
Table II - Emission Spectrographic Results for Specimen Gold.	26

LIST OF FIGURES

	<u>PAGE</u>
Fig. 1 - As-Received Microstructure of Gold Ribbon.	27
Fig. 2 - Microstructure of Annealed Gold Ribbon.	28
Fig. 3 - Substrate Plating Fixture.	29
Fig. 4 - Gold Ribbon and Gold Plated Substrate With Silver Markers Prior to Bonding.	30
Fig. 5 - Gold Ribbon and Gold Plated Substrate With Silver Markers After Bonding.	31
Fig. 6 - Bonded Specimen Showing Silver Markers Photographed With (Lower) and Without (Upper) Reference Mask Overlay.	32
Fig. 7 - Marker Motion Vs. Distance From Center for 230°C.	33
Fig. 8 - Marker Motion Vs. Distance From Center for 300°C.	34
Fig. 9 - Marker Motion Vs. Distance From Center for 370°C.	35
Fig. 10 - Marker Motion Vs. Distance From Center for 230°C Control and Contaminated Samples.	36
Fig. 11 - Marker Motion Vs. Distance From Center for 370°C Control and Contaminated Samples.	37
Fig. 12 - Marker Motion Vs. Distance From Center for Two Ribbon-Two Substrate System Bonded at 265°C.	38
Fig. 13 - Schematic Illustration of Two Ribbon-Two Substrate System.	39
Fig. 14 - SEM Photograph of Gold Ribbon Surface.	40
Fig. 15 - SEM Photograph of Thin Substrate Metallization, (400X).	41
Fig. 16 - SEM Photograph of Thin Substrate Metallization, (1000X).	42
Fig. 17 - SEM Photograph of Thick Substrate Metallization.	43

LIST OF FIGURES
(CONTINUED)

	<u>PAGE</u>
Fig. 18 - Schematic Illustration of Marker Motion Vs. Distance From Center as Predicted by Slip-Line Plasticity Theory.	44
Fig. 19 - Surface Strain Vs. Height Reduction for Thermocompression Bonded Specimens.	45
Fig. 20 - Contaminated (Lower) and Non-Contaminated (Upper) Samples Bonded at 370°C.	46
Fig. 21 - Photomicrograph of Two Ribbon-Two Substrate System Bonded at 265°C and 845 lbs. Force.	47

Abstract

A .062 inch x .010 inch x .375 inch gold ribbon was pressed against a gold plated rigid substrate with a flat overhanging tool to model lead attachment to thin film circuits. Experiments were conducted over a temperature range of 230°C to 370°C and a force range of 500 lbs. to 1000 lbs. resulting in height reductions of 5 to 17%. Silver markers, electrodeposited into grooves etched into both surfaces of the interface, were utilized to determine the elongation of both surfaces and relative movement between surfaces. Geometric effects were investigated by varying the thickness of the plated gold on the substrates, and conditions of symmetry were imposed by bond couples consisting of two of the .062 inch x .010 inch x .375 inch gold ribbons. Surface contamination was investigated by applying fingerprints onto specimens prior to bonding. After bonding the contaminated specimen data were compared to those of a control specimen.

Interfacial sliding was found to be of little importance to bond formation unless it prevented the inducement of deformation into the substrate metallization. Surface contamination had little effect on sliding for lower bonding temperatures, but for higher temperatures the amount of sliding was substantial. Surface contamination severely degraded bonds at both low and high bonding temperatures. Extension of both surfaces at the interface is necessary for bond formation. However, the amount of extension may be significantly reduced by the simultaneous application of interfacial shear.

I. INTRODUCTION

Solid phase welding, the welding of solid state materials with the absence of any liquid or gaseous phases, comprises a broad category of material joining techniques of which thermocompression bonding is included. Tylecote,¹ and Milner and Rowe² have reviewed the principles and possible mechanisms involved in solid phase welding. Investigations into the optimization of bond parameters and methods involved in the fabrication of electronic circuits have been undertaken by Joshi,³ Anderson, Christensen and Andreatch,⁴ Adams and Bonham,⁵ Deutsch,⁶ and Clark.⁷

Thermocompression bonding⁸ is the method by which two metals or a metal and a semiconductor, each in their solid phase may be joined together by the simultaneous application of heat and pressure such that at least one member undergoes deformation. Extensive use is made of thermocompression bonding in the electronics industry for hybrid integrated circuit fabrication. Electrical and mechanical connections between the integrated circuit gold beam leads and the substrate metallization are achieved by bringing the leads and substrate to some elevated temperature, normally between 250°C and 550°C, and applying sufficient force to deform the beam lead.

Anderson, Christensen and Andreatch⁴ developed the techniques of thermocompression bonding and performed preliminary investigations into bond formation between soft metal wires and semiconductors as a function of percent height reduction, bonding temperature and bonder tool geometry. Deutsch's⁶ studies were concerned with the

formation of thermocompression bonds between the metallized substrates and leads for external connection. Deutsch varied interfacial temperature, thin film metallization thickness and bonding force during the course of his experiments.

Clark,⁷ Ellington⁹ and Christensen¹⁰ all studied the effects of time, temperature and force on the formation of thermocompression bonds between semiconductor device leads or lead frames and metallized substrates.

Adams and Bonham⁵ investigated bonds formed by the wobble tool thermocompression bonding technique while varying force, time, temperature and sample cleanliness. They found that samples which had not been subjected to a cleaning process shortly before bonding had a bond failure rate three times that of the cleaned sample.

English and Hokanson¹¹ varied bonding tool temperature and force while thermocompression bonding gold plated copper lead frames to gold metallized ceramic and sapphire. Additionally, experiments were performed to determine the effects of heat treatment on bond quality. The results of the heat treatment experiments indicated that heat treatments prior to bonding were not beneficial and in some cases were detrimental to bond quality. However, a post bond heat treatment at 300°C for one hour did increase the bond quality.

Agers and Singer¹² measured the magnitudes of interfacial extension for lap welded aluminum sheets having various tool width

to sheet thickness ratios and different amounts of reduction in height or indentation. Interfacial extension was determined by observing the pattern of broken surface oxides along the interface. Agers and Singer only investigated the joining of sheets of equal thickness where sliding or relative movement between the two surfaces would not be expected to occur.

Joshi³ studied ultrasonic bond formation between gold, copper and aluminum wires with both similar and dissimilar substrates. Joshi varied power, force and time in his experiments and measured interfacial motion using a laser interferometer technique described by Martin and Wilson.¹³ Joshi concluded that for ultrasonically bonded samples there was no detectable relative motion along the interface between the wire and the substrate, and interfacial motion was not required for the formation of acceptable ultrasonic bonds. Chen¹⁴ also discussed the role of slip or sliding along the interface of ultrasonically bonded systems of aluminum and gold. Chen, referring to work performed by Mindlin et al.¹⁵ stated that micro-slip (slip on the order of one micrometer) was advantageous to bond strength, but that slip on a larger scale was detrimental to bond formation and produced irregular and unreliable bonds.

Dries,¹⁶ performing work preceding this investigation, characterized deformation and structural changes along the interface of gold-gold thermocompression bond couples by placing silver markers into one side of the interface. While this technique allowed him to determine the amount of deformation and surface elongation along

one side of the interface it did not provide a means of measuring relative motion and surface extension along both sides of the interface.

The author knows of no experimental data concerning interfacial sliding and surface strain along both sides of a thermo-compression bond interface though they are presumed to be important to the formation of a solid state bond as discussed by Tylecote, and Milner and Rowe² for example.

The intent of this investigation was to measure the degree of surface strain and interfacial sliding of gold-to-gold couples having undergone thermocompression bonding operations using different specimen geometries and bonding parameters. The study was accomplished by placing silver markers into grooves which were etched onto both surfaces of the interface and using optical and scanning electron microscopy to obtain the experimental results.

II. EXPERIMENTAL PROCEDURE

Interfacial sliding between gold surfaces during thermo-compression bonding was investigated by direct measurement of the relative motion of markers placed in the elements of a bond couple. In all experiments at least one of the elements was a 99.99% pure* gold ribbon having the following dimensions (0.010 in.) X (0.062 in.) X (0.375 in.). The gold ribbon was purchased from Englehard, Inc., Newark, New Jersey and was the same stock as was used by Dries.¹⁶ Prior to usage, the gold ribbon was annealed at 200°C in a circulating air furnace for 30 minutes, then allowed to cool in ambient temperature air. Figures 1 and 2 show the as-received and annealed microstructures, respectively. Generally the other element of the bond couple was a gold plated rigid steel substrate. The 0.075 inch steel substrates were cut from (0.025 in.) X (0.50 in.) Starret spring-tempered tool steel. The steel substrates were washed in boiling trichlorethylene followed by warm trichlorethylene, acetone, ethyl alcohol and then dried with nitrogen gas. The substrates were positioned within the nylon plating fixture shown in Fig. 3, and placed into a (100mm) X (50mm) Pyrex dish containing 200cc of continuously aggitated gold potassium cyanide plating solution which had been previously heated to 60°C. A 99.99% pure gold anode was placed into the plating solution and connected to the positive terminal of a direct current power source. The steel substrate was connected to the negative terminal. Plating currents and times on

*See Table II

the order of 5 milliamps and two hours produced plated gold thicknesses of approximately 0.7 mils.*

After the desired plated gold thickness had been achieved, the substrate was removed from the plating solution and fixture and rinsed in de-ionized water followed by a rinse in ethyl alcohol and dried with nitrogen gas. A 30 minute bake at 50°C was given to the substrate to provide better adhesion between the plated gold and the steel.

The following discussion pertains to marker generation in both the plated gold substrate and the gold ribbon. After the sample was cleaned, dried and baked, a thin film (approximately 3um) of Shipley AZ1350H positive type photoresist was applied to one surface using a Plat Engineering Company Model 102 spinner. The photoresist was further dried by heating the sample to 50°C in a circulating air furnace for 30 minutes then exposed through a pattern generation mask by a high intensity mercury vapor light source. The sample was then placed into a Shipley AZ developing solution which removed the exposed photoresist thereby creating the desired marker pattern. The marker pattern was etched to an approximate depth of 4um by immersion into a solution of potassium iodide and iodine for one and one-half minutes. A Leitz split beam microscope was used to measure the depth of the etched marker pattern.

Following the etching process, the sample was placed into a silver plating solution composed of silver nitrate, ammonium hydroxide
*1 mil = .001 inch = .0254mm.

and ammonium sulfate. Silver was then deposited into the etched markers on the surface of the sample. A maximum plating time of 4 seconds was required to avoid over filling the 4um deep marker grooves. Figure 4 shows the marker patterns on a typical substrate and ribbon prior to the bonding operation.

All of the couples were thermocompression bonded using the modified Keller lab bonder described by Dries.¹⁶ The modifications to the bonder were the following, 1) addition of Victor Controls high volume, fast activating control valves which resulted in 40 millisecond rise and fall times for load application and removal, 2) installation of Statham Model UC3 load cell and Model UR5 universal transducer readout which gave instantaneous readout of applied force, 3) instantaneous height measurement capability provided by addition of Hewlett-Packard Series 7DCDT displacement transducer. The Statham load cell and universal transducer readout were calibrated using a Instron compression cell which was calibrated using known weights. The Hewlett-Packard displacement transducer was calibrated using shim stock of various thicknesses. Both the load cell and displacement transducer were connected to a Tektronix Model 564 dual trace, storage oscilloscope. The oscilloscope traces were calibrated to correspond to the load cell (force transducer) and to the displacement transducer outputs.

The bonder was equipped with two thermodes (Type 303 stainless steel) which were fitted with cartridge type electric heaters. The temperature of each thermode was controlled by separate temperature

controllers which sensed the thermode temperatures by means of a chromel-alumel thermocouple placed between the cartridge heater and the thermode. The thermal gradient across the two thermodes was minimized by adjusting both of the thermodes to the desired interface temperature. A Hewlett-Packard Model 7100B strip chart recorder and a chromel-alumel thermocouple were used to monitor the thermode temperatures. The individual thermode temperatures were obtained by placing a 0.125 inch thick section of asbestos between the two thermodes and inserting the thermocouple between the asbestos and the thermode of interest. This technique was applied alternately between the two thermodes until their temperatures were equal and at the desired interface temperature.

A thin foil* chromel-alumel thermocouple was bonded between a gold ribbon and a gold plated steel substrate to confirm that the actual interface temperature of the sample during the bonding process was not significantly different from that of the thermodes. The interface-thermode temperature differential was found to be less than 2% at 300°C. Bond dwell time, the time that the force was applied to the bond couple, was controlled by a Lektra Model TM-8 electronic decade interval timer. All experiments were conducted using a 6 second dwell time.

Following force calibration and adjustment of the time and temperature controllers to the desired values, the bonder was ready for use. The gold ribbons and metallized substrates were placed between the thermodes, and a section of shim stock having

*0.5 mils thick.

a thin plating of gold (< .05 mils) was placed on top of the ribbon to insure uniform sticking friction from sample to sample. After bonding, all samples were removed from between the thermodes and immediately quenched into cold water. It is estimated that samples were quenched within 3 seconds of the release of the bond force. Figure 5 shows a gold ribbon bonded to a gold plated steel substrate. The steel substrates were removed by etching the samples in a 50% HCL, 50% water (by volume) solution. The substrate removal was necessary to prevent cathodic protection of the gold during etching. The bonded sample with the steel substrate removed was cut, normal to the length of the ribbon, into two equal pieces which were prepared for metallography. Both halves of the sample were mounted in the same epoxy specimen holder so that the markers could be found more easily.

The sample was ground down until a set of markers was located. Then standard metallographic procedures were employed to polish the sample. Photographs of the samples were taken through the negative of the mask used to generate the markers (see Fig. 6), and the movement of the markers relative to their neighbors was then determined.

The plated gold thickness and the percent height reduction due to bonding were determined by means of a Leitz metallograph and a calibration standard having lines on 0.001 inch centers. Photographs were taken at 500X of both the edge of the plated gold and the calibration standard. The plated gold thickness was determined

by comparing the two photographs. Similarly, the percent height reduction was determined using 200X photographs. A detailed description of the composition and operating characteristics of the plating baths and the photolithic procedure used to generate the markers on the sample surfaces may be found in the appendices of Dries¹⁶ thesis.

III. RESULTS AND DISCUSSION

The deformation of the two surfaces at the bond interface and the amount of relative movement between them is defined by the marker experiments just described. There are several parameters that may be of interest. One is the amount of relative movement or sliding between the two surfaces, δ , another is the degree of marker motion, u , and a third is the surface strain, e .

Interfacial sliding is the movement of a surface on one side of an interface as compared to the movement of a surface on the opposite side of the interface. Silver markers placed into each surface of the interface were used to determine the degree of interfacial sliding.

Marker motion is the net displacement of markers as compared to their original spacings. Figure 6 shows a section of a bonded specimen photographed with and without the reference mask overlay. By comparing the center-to-center distance between silver markers to that of the reference mask one can determine the amount of marker motion along both sides of the interface.

Surface strain is expressed using the engineering concept of strain as was used by Dries¹⁶ and is given by:

$$e = \frac{du}{dx}, \quad (1)$$

where, u , is the displacement from some point which was originally a distance, x , from some reference point. Surface strain corresponds to the slope of the marker motion (or displacement) vs. original position curves shown in Figs. 7 through 12.

The criteria used to plot the marker motion vs. original position curves were, 1) an assumption that marker motion and surface extension tend to be symmetric and 2) motion of markers in the substrate (the driven element) must be less than or equal to that of markers in the ribbon (the driving element) for a given distance from the center of the interface.

Experiments were conducted using bonding temperatures ranging from 230°C to 370°C and forces from 500 lbs. to 1000 lbs.. A six second bond dwell time was used throughout the study. Three different sets of circumstances were employed during the investigation and will be discussed in separate sections: A) samples bonded at 230°C, 300°C and 370°C utilizing at least two substrate plating thicknesses for each temperature, B) two sets of samples (one contaminated, one control) were bonded of 230°C and 370°C, C) symmetric conditions provided by ribbon-to-ribbon bonding configurations.

A. Varying Substrate Plating Thickness

Experiments were conducted with a 1000 lbs. bonding force and temperatures of 230°C, 300°C and 370°C utilizing two different substrate plating thicknesses for each temperature. The ratio of thick to thin plated gold thicknesses for a given experiment was approximately 2:1. Scanning electron microscope photographs of the rolled gold ribbon, thin plated gold and thick plated gold are shown in Figs. 14 through 17, respectively. The small crater shaped regions observable in Fig. 17 are due to chemical attack on

the thick plated gold during the marker generation process. Peaks or sharp ridges on the thick plated surfaces apparently had thinner than desirable photoresist coatings, and in some instances the barrier to the gold etchant was penetrated. The changed topography due to this etching of the thick metallization is not thought to have played a significant role in the thick-thin plating marker studies.

Figures 7 through 9 illustrate the differences in marker motion, surface strain (the slope of the curve) and interfacial sliding (the difference between the curves) between samples having thick and thin substrate metallizations. Each figure presents the data for a given bonding temperature. Figure 8 shows a comparison between three samples, each with a different metallization thickness (0.50 mils, 1.34 mils, 1.52 mils), which were bonded using the same bond parameters (300°C, 1000 lbs.). As the metallization thickness was increased, the marker motion, u , was observed to increase and the amount of interfacial sliding, δ , decreased. The slopes of the ribbon curves (corresponding to surface strain of the lead) for all three metallization thicknesses were approximately equal. However, the slopes of the substrate curves (corresponding to the surface of the substrate metallization) increased with increasing metallization thickness. Though there was a large difference in the amount of sliding for the three bond couples, there was no discernable difference in the extent of bond formation.

Marker motion near the center of symmetry of the thinner metallizations appeared to be significantly less than that corresponding to the thicker metallizations. This behavior is predictable from slip-line plasticity theory. Figure 18 illustrates a marker motion vs. distance from center curve with a "dead zone" region projected onto it from a slip-line field plot having a width to height ratio of 6.7.¹⁷ The horizontal line through the slip-line field represents a metallization thickness of approximately one mil, and it can be observed that for increasing metallization thicknesses the width of the "dead zone" decreases. This was seen to be the case for the thick-thin metallization experiments.

The 230°C thick and thin substrate samples (see Fig. 7) exhibited marker behavior similar to that observed for the 300°C samples except that marker movements and strains were about one-half those of the 300°C samples corresponding to the fact that height reductions were about one-half those of the 300°C samples. The 370°C samples, whose data are plotted in Figure 9, show a relatively high degree of marker motion for both thick and thin metallization thicknesses. Interfacial motion is indiscernible for both plating thicknesses, and the region of least motion (that region in close proximity to the center of the ribbon) was more narrow than was observed for lower temperature samples.

Figure 19, a plot of surface strain vs. height reduction, is composed of data obtained from the thick-thin substrate experiments. The surface strains were measured in the "plastic zone" of the curves as indicated on Fig. 18 and correspond to the surface strain of the ribbons. The three data points having the lowest value of surface

strain are for the 230°C samples, the center three are for the 300°C samples and the top three are for the 370°C samples. As a first approximation, the surface strain vs. height reduction plot may be taken as a straight line. However, there appears to be some higher order temperature effects which cause a departure from linearity.

B. Surface Contamination

The second series of experiments was concerned with the effects of contaminated surfaces. Two experiments were conducted to determine the effects of surface contamination (for the investigation a finger print was used as the contaminant) on interfacial sliding, surface strain and bond formation. Temperatures of 230°C and 370°C, and a 1000 lb. force were selected for these experiments. A non-contaminated* control specimen for each temperature was prepared and processed concurrently with the contaminated sample. The two sets of bond parameters were chosen to investigate whether the influence of surface contamination strongly depends on temperature or deformation.

The data plotted in Fig. 10 are from two samples which were bonded sequentially using the same conditions (230°C, 1000 lbs.). The upper set of curves are those of the control (non-contaminated) sample, and the lower set of curves are for the contaminated sample whose substrate had been rubbed between thumb and forefinger to produce a smeared fingerprint on its surface. The degrees of interfacial sliding for the two samples shown in Fig. 10 lie between

*Specimen that was not intentionally contaminated.

those of the thick (1.76 mils) and thin (.58 mils) substrate samples shown in Fig. 7. This was to be expected since the substrate thicknesses of the control and contaminated samples (.78 mils and .82 mils, respectively) are bracketed by those in Fig. 7, and all four samples exhibited similar height reductions (5.0 - 6.3%).

The data from the 370°C. samples are shown in Fig. 11. The difference in interfacial sliding between the 370°C contaminated (lower set of curves) and non-contaminated samples is much more pronounced than that of the 230°C samples shown in Fig. 10. For the 230°C thin substrate samples, the amount of sliding normally associated with a non-contaminated specimen is approximately the same as for a contaminated specimen. This does not imply that equal bonding was observed between the 230°C contaminated and non-contaminated samples. The non-contaminated sample bonded over approximately 90% of the interface while the contaminated sample bonded over only approximately 20% of the interface. At the higher temperature (370°C), there was less inherent interfacial sliding observed for the non-contaminated sample (upper set of curves in Fig. 11), but there was a significant amount of sliding along the interface of the contaminated sample. The bond region for the control sample was approximately 90% of the interface while that of the contaminated sample was approximately 20% of the interface. Both samples received similar height reductions (16.4% for the control and 15.3% for the contaminated) and the surface extensions seen in both ribbons were approximately equal, yet the degree of surface extension induced into the substrate was significantly

different. Due to the reduction in friction created by a fingerprint, the observed surface extension of the contaminated substrate was much less than that observed for the control substrate. The control substrate surface extension was equal to that of the control ribbon. Figure 20 shows a comparison between two samples which were bonded under the same bond parameters. The lower sample had been contaminated with a fingerprint and the upper sample was a control. The dashes along the interface of the control sample are the silver markers (note the marker located in the bonded region of the contaminated sample).

Contaminated surfaces do not contribute significantly to the degree of interfacial sliding observed for low temperature bonding situations, but surface contaminants do contribute to the degradation of the bond. For higher temperature bonding conditions, the presence of surface contamination significantly increases the amount of interfacial sliding in addition to severely degrading the bond.

C. Symmetric Conditions

A third series of experiments was conducted to determine the effects of imposed symmetric conditions on marker motion, surface strain and interfacial shear. Bond couples consisting of two metalized steel substrates and two gold ribbons were positioned so as to provide the following interface arrangement, 1) substrate-ribbon, 2) ribbon-ribbon, 3) and ribbon-substrate. The four element bond couple is illustrated schematically in Fig. 13. For this configuration there was no interfacial shear stress between the two ribbons due to

symmetry. When the sample was thermocompression bonded at 265°C with an 845 lbs. force, there was almost complete bond formation along both ribbon-substrate interfaces (AB and CD on Fig. 13), but the bonded area covered only about 5% of the ribbon-ribbon interface (BC on Fig. 13). The total height reduction for this sample was approximately 12%, and the surface strain along the ribbon-ribbon interface was about 20%. Experiments using temperature and force combinations of 230°C-500 lbs., 230°C-860 lbs., 230°C-1000 lbs. and 265°C-535 lbs. did not provide bonds between two ribbons. Repeated experiments with temperature and force combinations of 300°C-500 lbs. and 265°C-845 lbs. resulted in partial bonding at least once for each of the combinations.

In an attempt to eliminate the topography differences between the ribbon-ribbon interface and the ribbon-substrate interfaces, one of the gold ribbons was electroplated with gold in order to make its topography similar to the gold metallized substrate. A photomicrograph of the plated ribbon sample is shown in Fig. 21. The ribbon-ribbon interface was slightly displaced from the center of symmetry due to the inadvertent pairing of the thicker plated ribbon with the thicker substrate metallization. The two ribbon and two substrate system was bonded using an 845 lbs. force at 265°C as was used previously. The resulting height reduction was 11.8% and the surface strain along the ribbon-ribbon interface was approximately 25%. Again both ribbon-substrate interfaces formed good bonds. Bond formation along the ribbon-plated interface increased to approximately 30% of the interface length.

The effect of symmetry was investigated while attempting to bond two gold ribbons. Bond parameters which provided bonds between gold metallized steel substrates and gold ribbons were not adequate to form bonds between two gold ribbons even though there was more surface elongation. Electroplating one of the gold ribbons increased the extent of bonding along the ribbon-ribbon interface.

IV. SUMMARY AND CONCLUSIONS

Experiments were conducted to determine the effects of metallization thickness, surface contamination and shear stress on extension of surfaces, sliding and bond formation at gold-gold interfaces. The movement of material during bonding was observed by the use of silver markers which were deposited in shallow grooves in both of the surfaces forming the interface. Couples were bonded using temperature and force combinations ranging from 230°C to 370°C and 800 lbs. to 1000 lbs.

Marker motion in the ribbon was generally reproducible, independent of substrate metallization thickness and increased approximately linearly with increasing height reduction. For thin substrate metallizations, there was a region where there was little marker movement which correlated with a dead-zone predicted by slip-line plasticity theory and bonding difficulty.

Interfacial sliding appeared to be deformation independent and varied inversely with bonding temperature and substrate metallization thickness. More sliding was observed for samples having lower bonding temperatures, thinner substrate metallization thicknesses and contaminated surfaces. Since marker motion in the ribbon was not strongly temperature or contaminant dependent and sliding was, marker motion at the surface of the metallization was much less than ribbon motion for sliding conditions. There was considerable sliding observed for samples bonded at 230°C with little difference between contaminated and uncontaminated samples. At 370°C, there was still considerable sliding observed for the contaminated sample but negligible sliding for the control sample. Although there was little

sliding difference observed for the 230°C samples, surface contamination severely degraded bond formation for both the 230°C and 370°C contaminated samples.

The surface strain of both ribbons (leads) and substrate metallization increased with increasing deformation. Metallization thickness had little effect on the magnitude of ribbon surface strain in the plastic zone, but increased metallization thickness did act to decrease the extent of the apparent dead-zone. Surface strain of the substrate metallization approached that of the ribbon for the thicker, non-contaminated metallization samples. When sliding occurs due to contamination, a lower temperature or thinner substrate metallizations, there is a corresponding reduction in the amount of surface extension of the substrate metallization.

There seemed to be no strong correlation between bond formation and the amount of interfacial sliding since bonding occurred with no detectable sliding and with sliding of about 1 mil. The amount of extension induced along the substrate metallization surface seemed to be the important factor in bond formation. All of the experiments seem consistent with an interpretation that sliding is unimportant unless sliding occurs at such a low shear stress that extension is not induced into the substrate metallization. In other words, the coefficient of friction must be high enough, or seizure must occur at enough contact points to induce deformation of substrate metallization and further seizure. This view is supported by work by Antle,¹⁸ who optimized thermocompression bonding parameters (cleaning techniques, atmospheres, choice of couple materials, and

temperature) using a friction measuring technique. A coefficient of friction viewpoint makes the contaminated and uncontaminated results clearer. At 230°C, the presence of the contaminant did not alter the coefficient of friction significantly resulting in similar marker behavior. However, the contaminant did inhibit bond formation. At 370°C, the contaminant strongly influenced the coefficient of friction and inhibited bond formation.

Minimization of interfacial shear stress, accomplished by imposing symmetric conditions, resulted in a failure to form bonds when parameters which were normally adequate for bond formation were employed. Electroplating one surface of the symmetric interface resulted in a partial bond, yet the bonded region of the interface was still less than 30%. Bond formation may occur by the extension of two bond surfaces, but the amount of extension required in the absence of shear is rather high. If shear stress is applied during bonding, the amount of surface extension required for bond formation is reduced. It appears that there can be bond formation with no surface extension, or even some contraction, as shown in Fig. 7, if local shear strains occur. Though the bonding experiments comparing bonding under symmetric and asymmetric conditions show that the amount of surface extension required for bonding is reduced by the simultaneous application of a shear stress, there have not been enough experiments performed to define the threshold conditions for bond formation in terms of surface extension, shear, temperature and time. However, if the shear stress can be calculated from

plasticity theory, it should be possible to determine the threshold conditions without the necessity of using markers since the surface extensions are reasonably well behaved.

In conclusion, the present investigation of gold-gold thermo-compression bond formation indicates that:

- 1) extension of both surfaces at the interface is necessary for bond formation,
- 2) sliding is unimportant except when it can occur so easily that deformation is not induced at the surface of the substrate metallization,
- 3) the simultaneous presence of interfacial shear significantly reduces the amount of surface extension required for bond formation even to the extent of overcoming slight surface contractions, and
- 4) the presence of a contaminant can inhibit bond formation even though surface extension of both contaminated and uncontaminated surfaces appeared to be the same.

Sample No.	BOND PARAMETERS			SPECIMEN PARAMETERS (in. X10 ⁻³)				
	Time (sec.)	Temp. (°C)	Force (lbs.)	Plating Thick.	Initial Height	Final Height	Height Red. %	% Bond Formed
15	6	230	1000	0.589	10.589	10.0	5.6	>90
6	6	230	800	1.11	11.11	10.5	5.5	>85
16	6	230	1000	0.58	10.58	10.05	5.01	>90
23	6	230	1000	2.47	12.47	11.85	5.00	<50
26	6	230	1000	0.78	10.78	10.10	6.31	>90
27	6	230	1000	0.82	10.82	10.15	6.19	<50
7	6	300	1000	0.316	10.316	9.63	6.6	>90
8	6	300	1000	0.368	10.368	9.63	7.1	>90
12	6	300	1000	1.34	11.34	10.0	11.5	>90
18	6	300	1000	0.50	10.5	9.5	9.52	>85
20	6	300	1000	1.52	11.52	10.5	8.85	>90
2	6	370	800	0.737	10.737	9.84	8.4	>80
5	6	370	1000	1.00	11.00	8.42	23.5	>90
9	6	370	1000	0.368	10.368	9.58	7.6	>90
10	6	370	1000	0.632	10.632	9.42	11.4	>80
11	6	370	1000	1.37	11.37	10.42	8.4	>75
13	6	370	1000	0.90	10.90	9.6	11.93	>90
14	6	370	1000	0.895	10.895	9.53	12.5	>90
22	6	370	1000	1.66	11.66	10.15	12.95	>90
24	6	370	765	0.82	10.82	9.05	16.36	>90
25	6	370	765	0.92	10.92	9.25	15.3	<20
28	6	370	610	0.632	10.632	10.16	4.4	<20

TABLE I

Bond and Specimen Parameters.

TABLE II

Emission Spectrographic Results for Specimen Gold

<u>SAMPLE</u>	<u>PRIMARY ELEMENT</u>	<u>% Ag</u>	<u>% Cd</u>	<u>% Al</u>	<u>% Cu</u>	<u>% Fe</u>	<u>% Ni</u>	<u>% Pb</u>	<u>% Mg</u>	<u>% Pd</u>	<u>% Si</u>
A	Au	<.01	<.005	<.001	<.001	<.001	<.001	<.001	<.0001	N.D.	N.D.
B	Au	<.01	N.D.	<.001	<.01	<.001	N.D.	<.001	<.0001	<.01	N.D.
C	Au	<.01	N.D.	<.001	<.01	<.001	N.D.	<.001	<.0001	N.D.	N.D.
D	Au	<.01	N.D.	<.001	<.01	<.001	N.D.	<.001	<.0001	<.01	<.001

Sample A - Electroplated Gold Foil

Sample B - Gold Ribbon Previously Bonded to Sample A

Sample C - Gold Ribbon From Stock

Sample D - Gold Ribbon Previously Bonded to Another Gold Ribbon

N. D. - None Detected

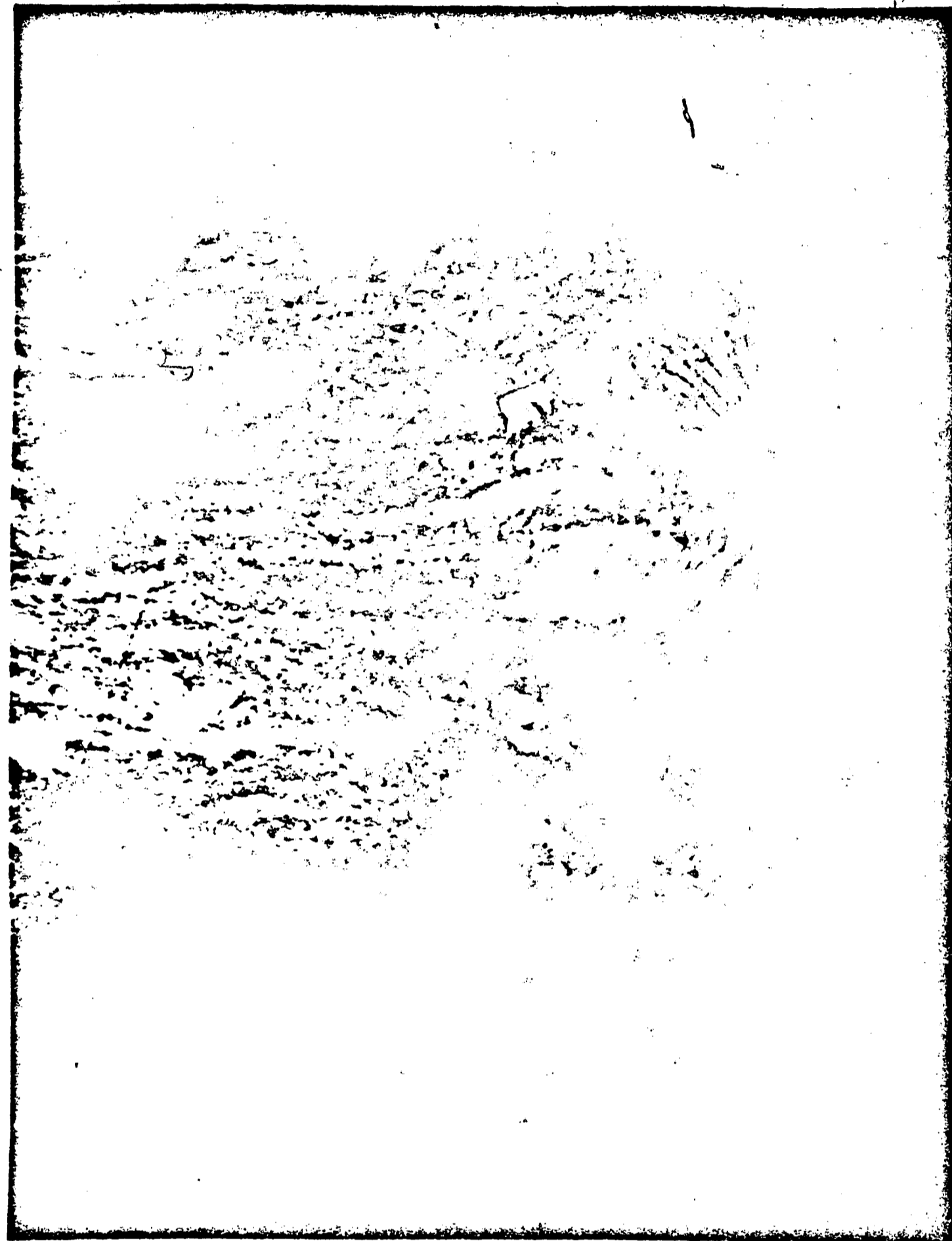


FIG.1 AS - RECEIVED MICROSTRUCTURE OF GOLD RIBBON.
(200X)

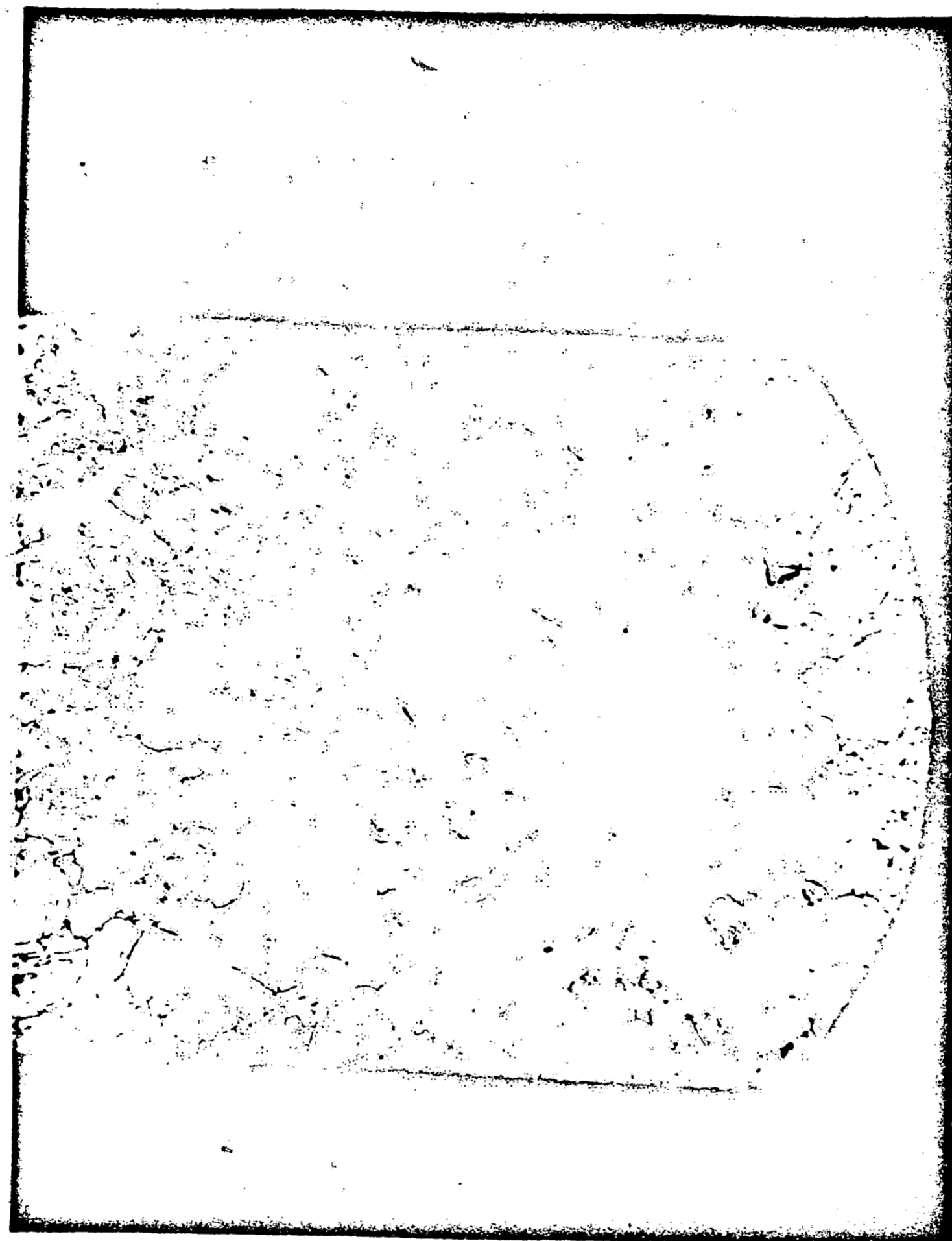


FIG. 2 MICROSTRUCTURE OF ANNEALED GOLD RIBBON. SPECIMEN WAS
ANNEALED FOR ONE - HALF HOUR AT 300°C.
(200X)

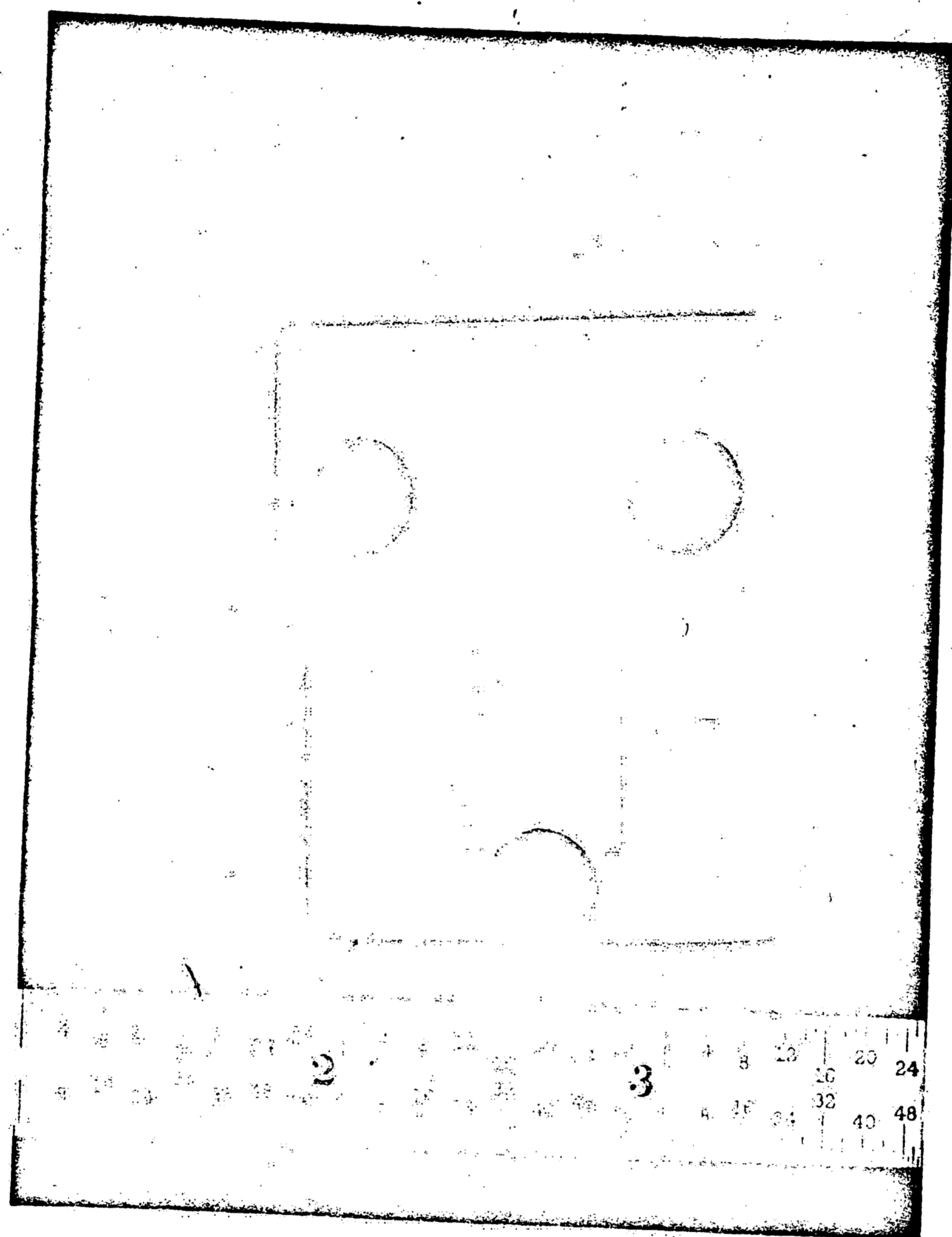


FIG. 3 SUBSTRATE PLATING FIXTURE

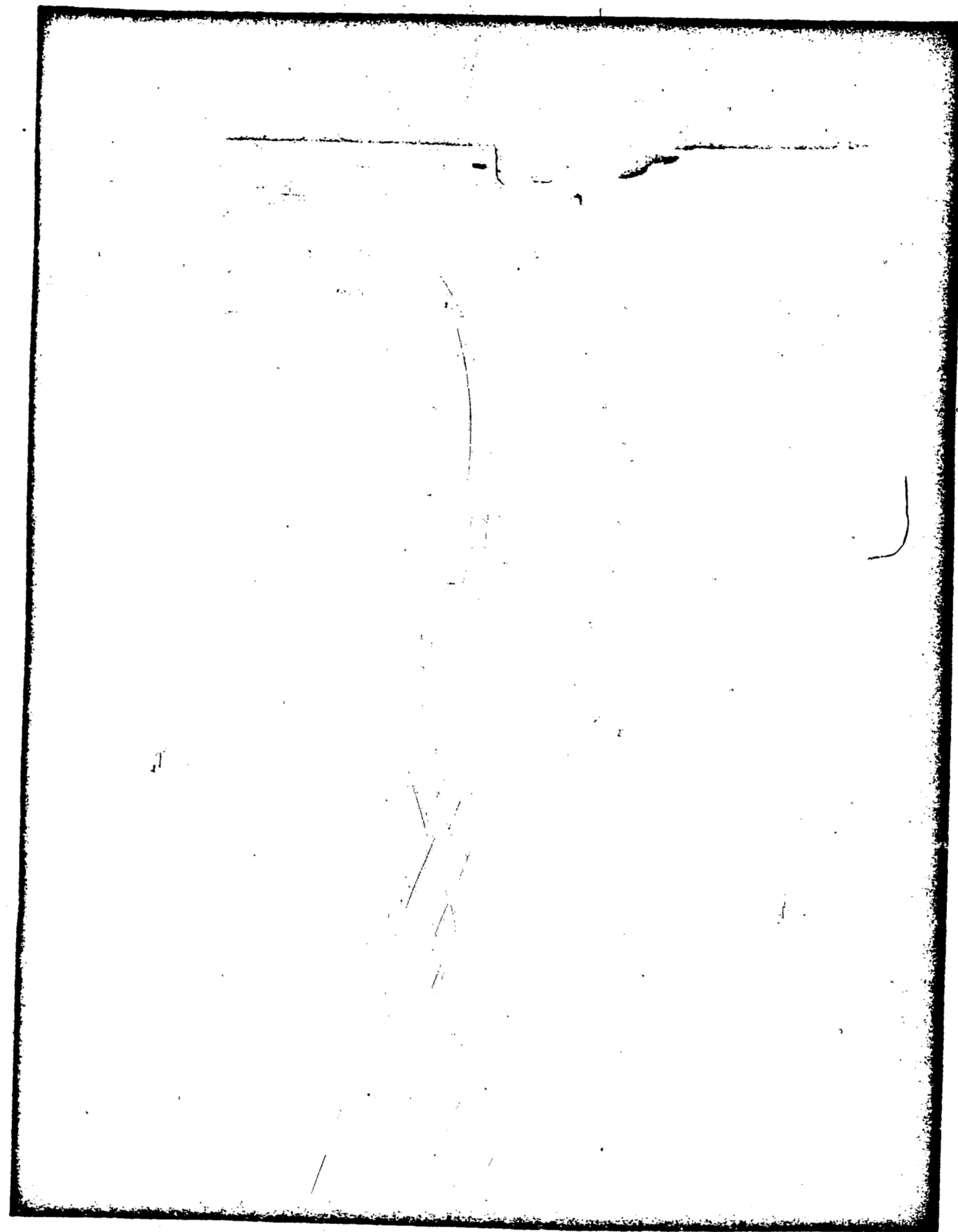


FIG. 4 GOLD RIBBON AND GOLD PLATED SUBSTRATE WITH SILVER MARKERS
PRIOR TO BONDING.

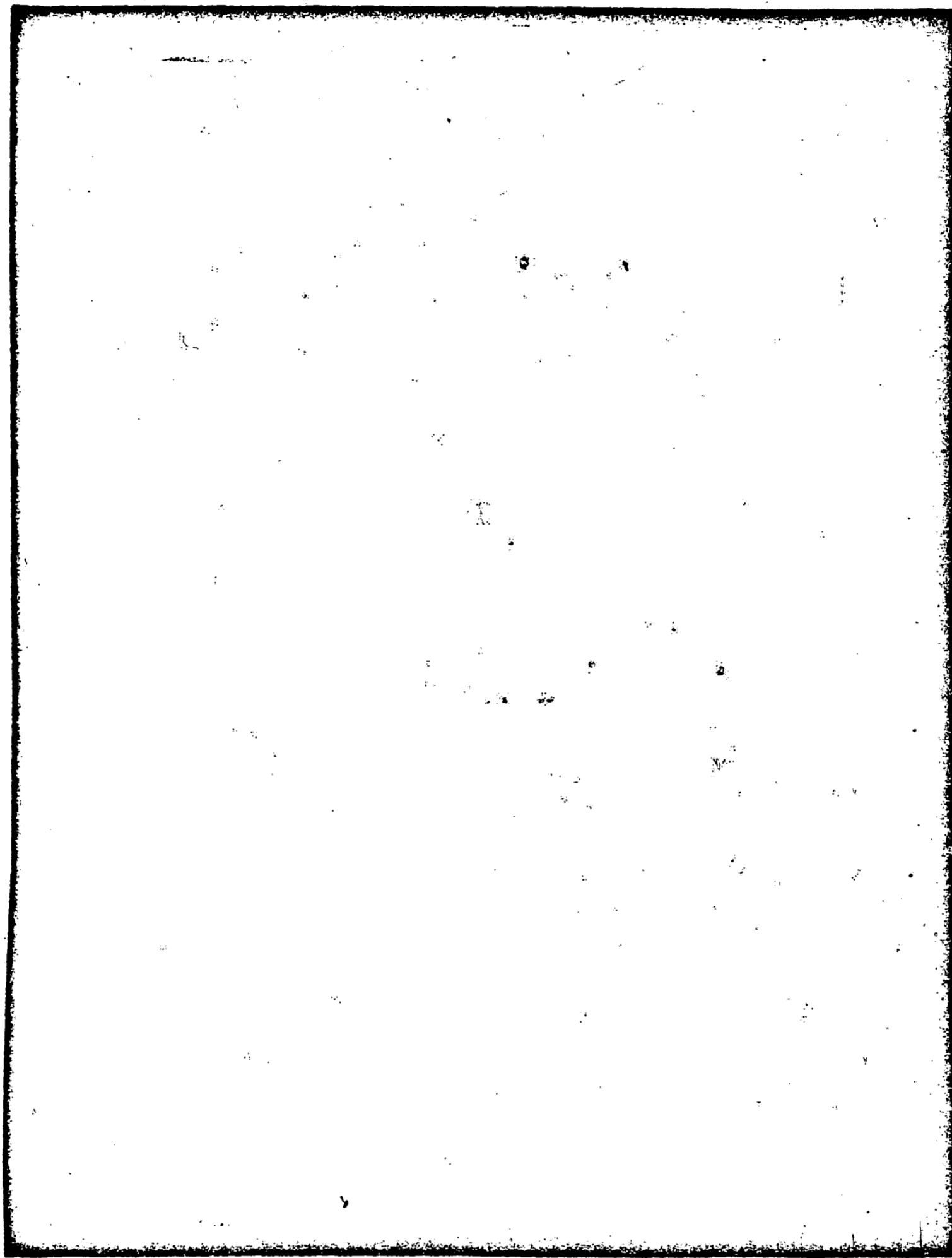


FIG. 5 GOLD RIBBON AND GOLD PLATED SUBSTRATE WITH SILVER MARKERS
AFTER BONDING.

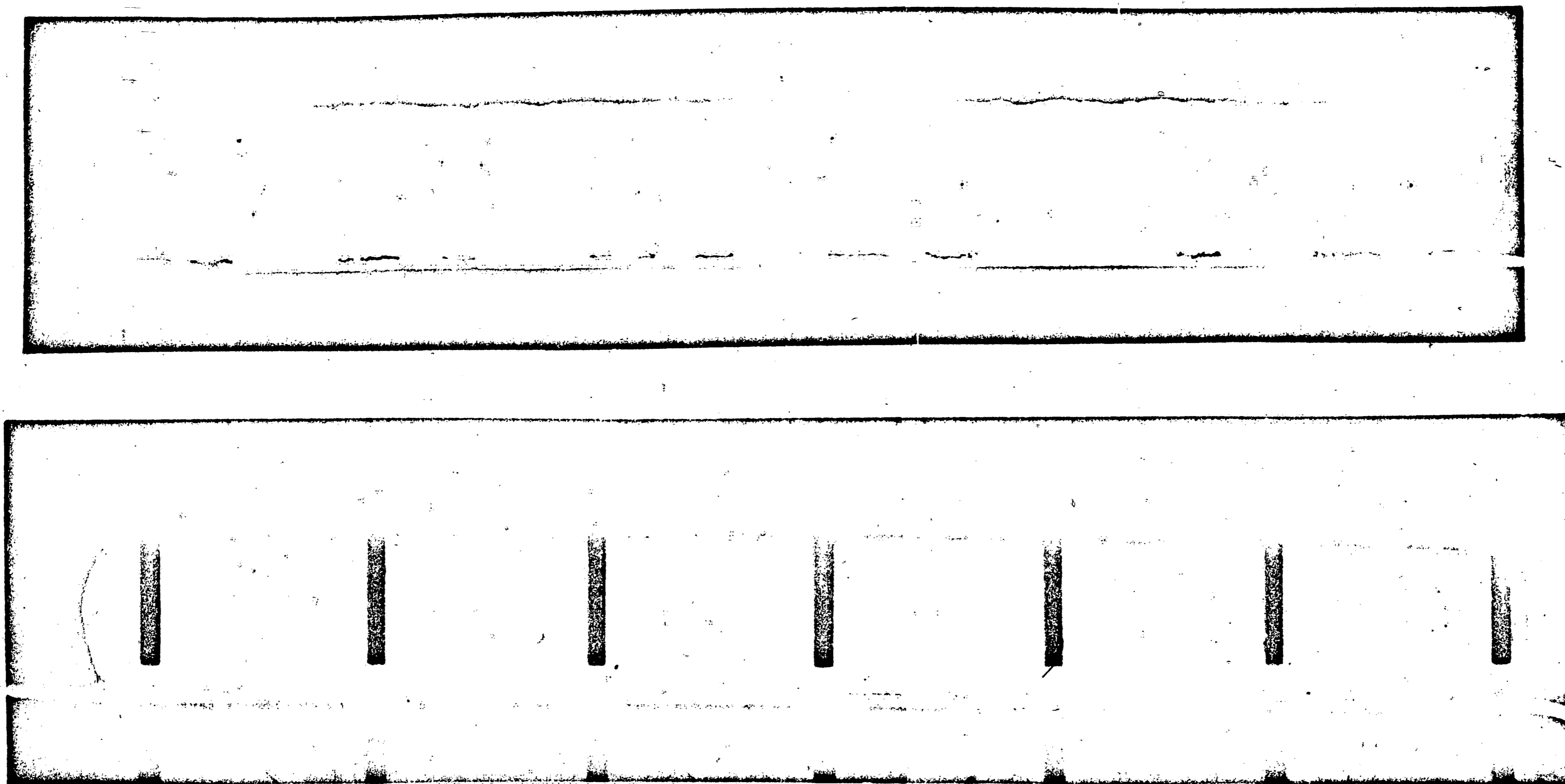
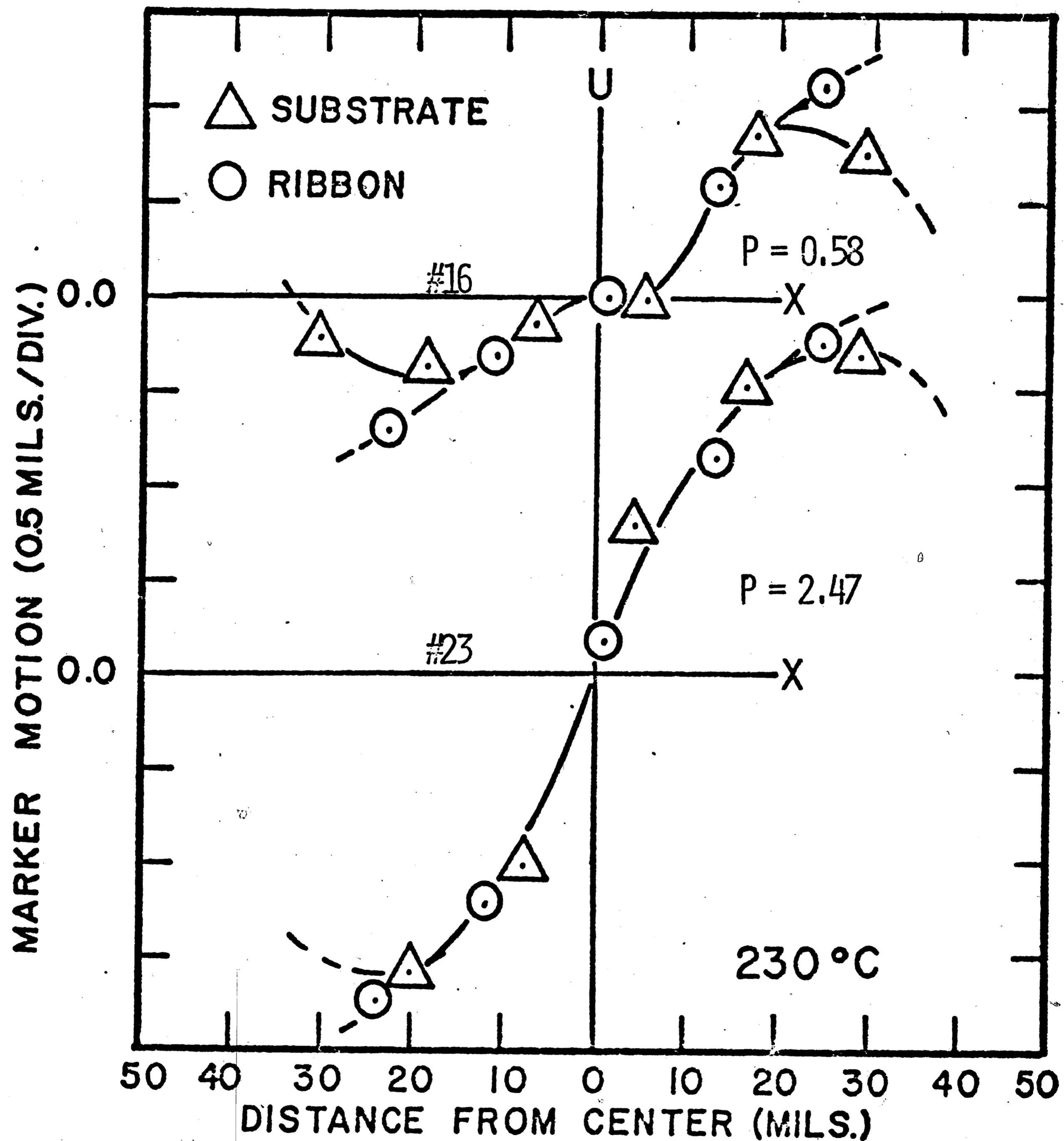


FIG. 6 BONDED SPECIMEN SHOWING SILVER MARKERS PHOTOGRAPHED WITH (LOWER) AND WITHOUT (UPPER) REFERENCE MASK OVERLAY (100X).



NOTE: P = SUBSTRATE METALLIZATION THICKNESS IN MILS.

FIG. 7 MARKER MOTION VS. DISTANCE FROM CENTER FOR 230°C

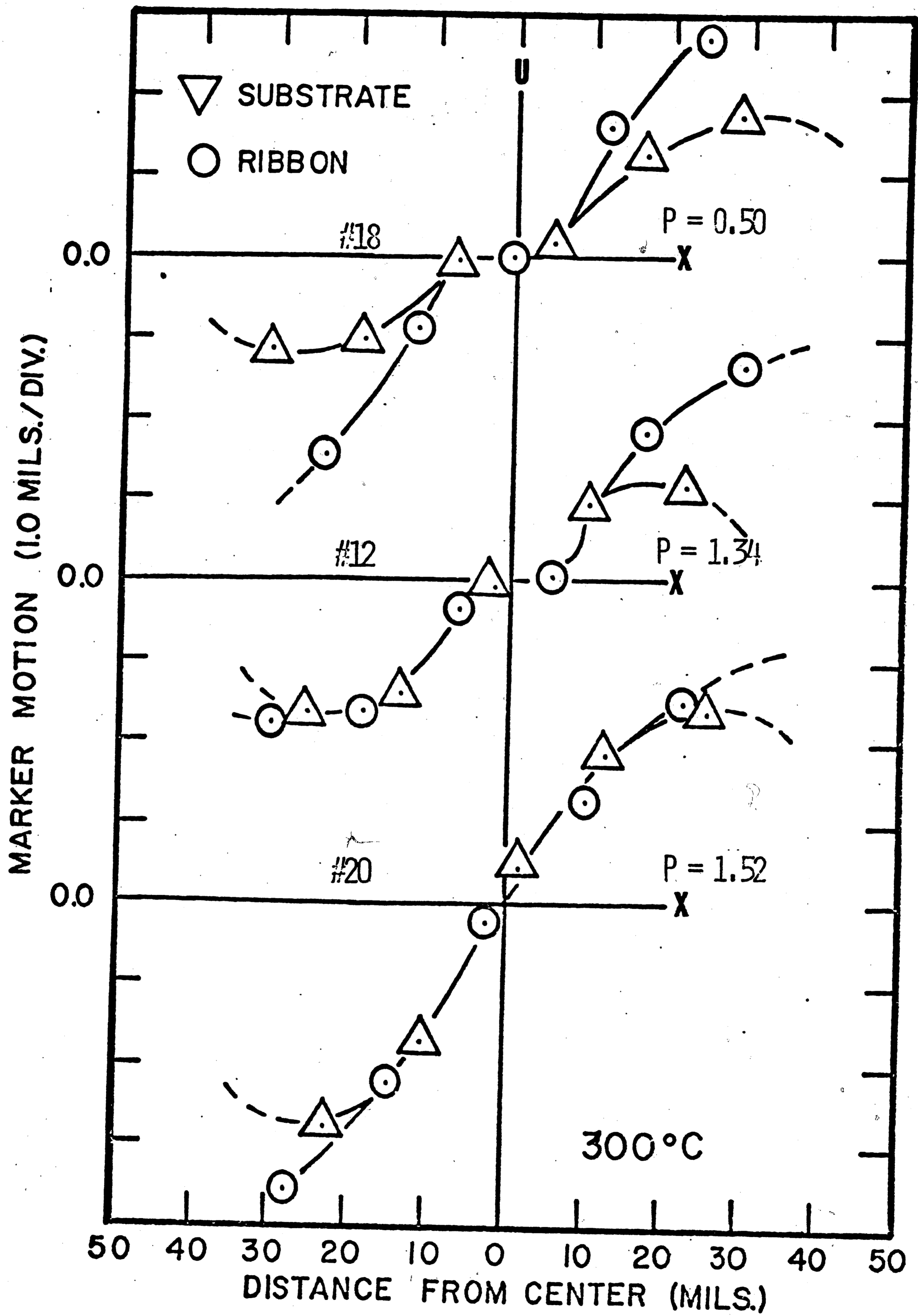


FIG. 8 MARKER MOTION VS. DISTANCE FROM CENTER FOR 300°C.

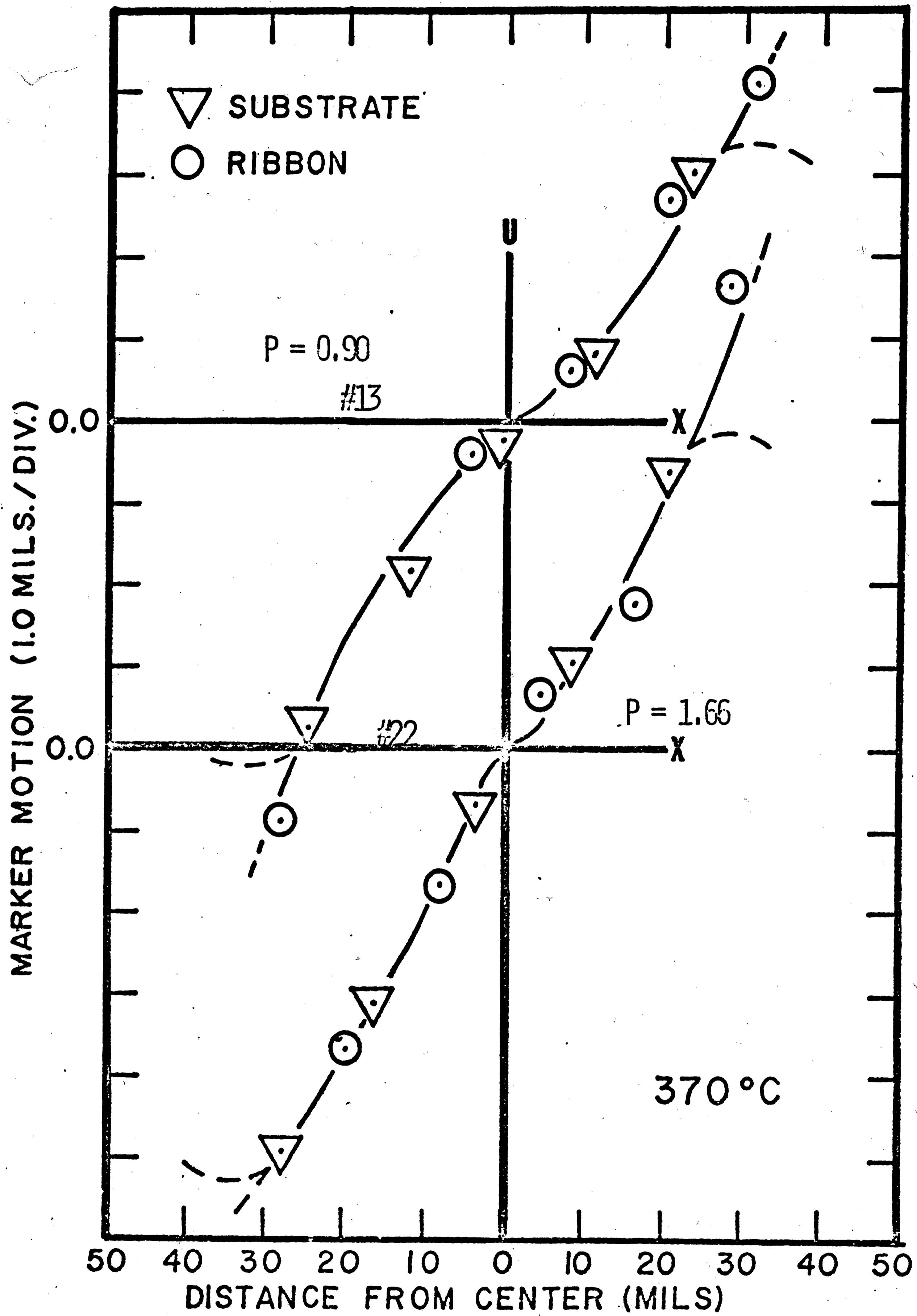


FIG. 9 MARKER MOTION VS. DISTANCE FROM CENTER FOR 370°C.

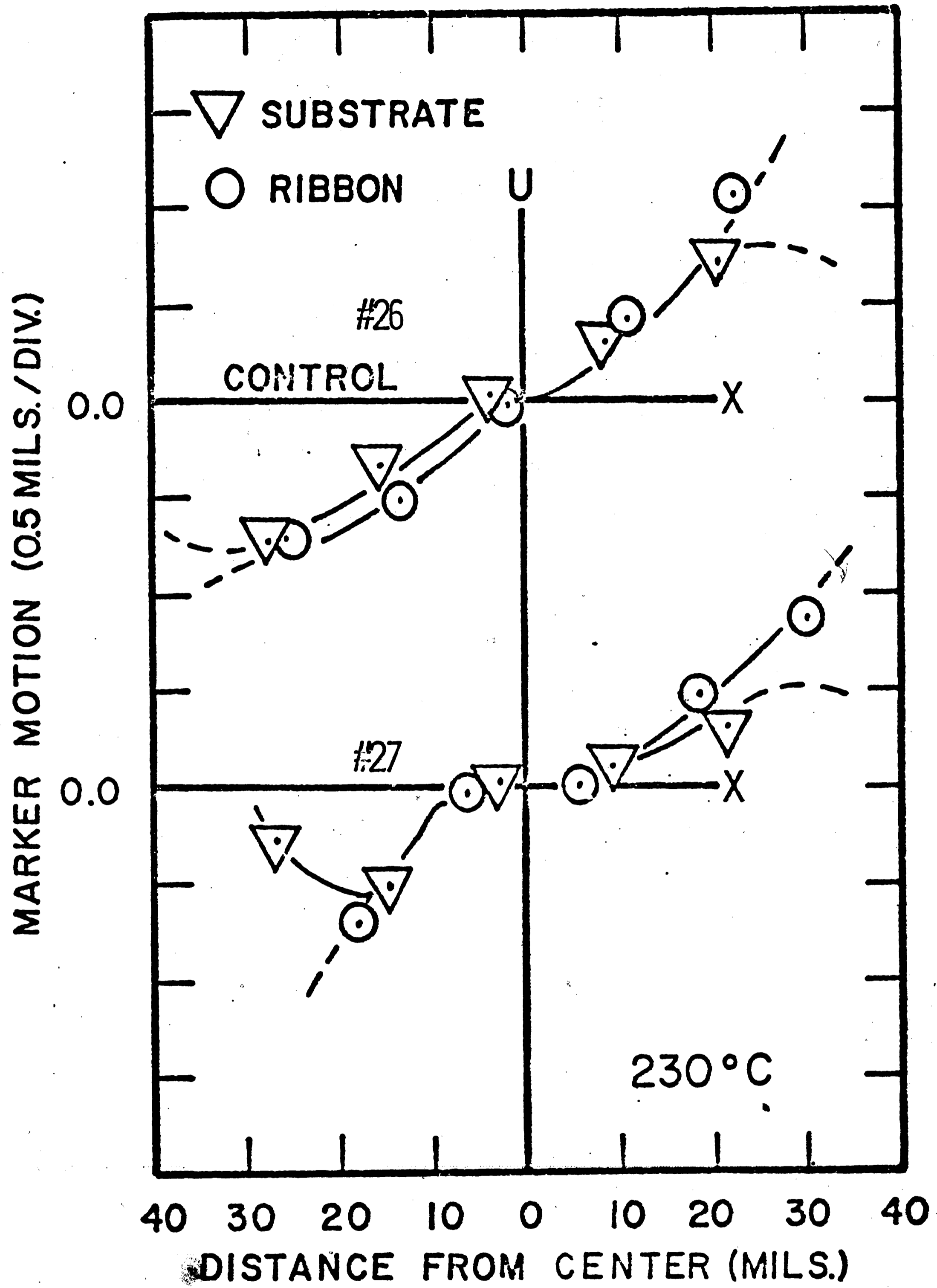


FIG. 10 MARKER MOTION VS. DISTANCE FROM CENTER FOR 230°C CONTROL AND CONTAMINATED SAMPLES.

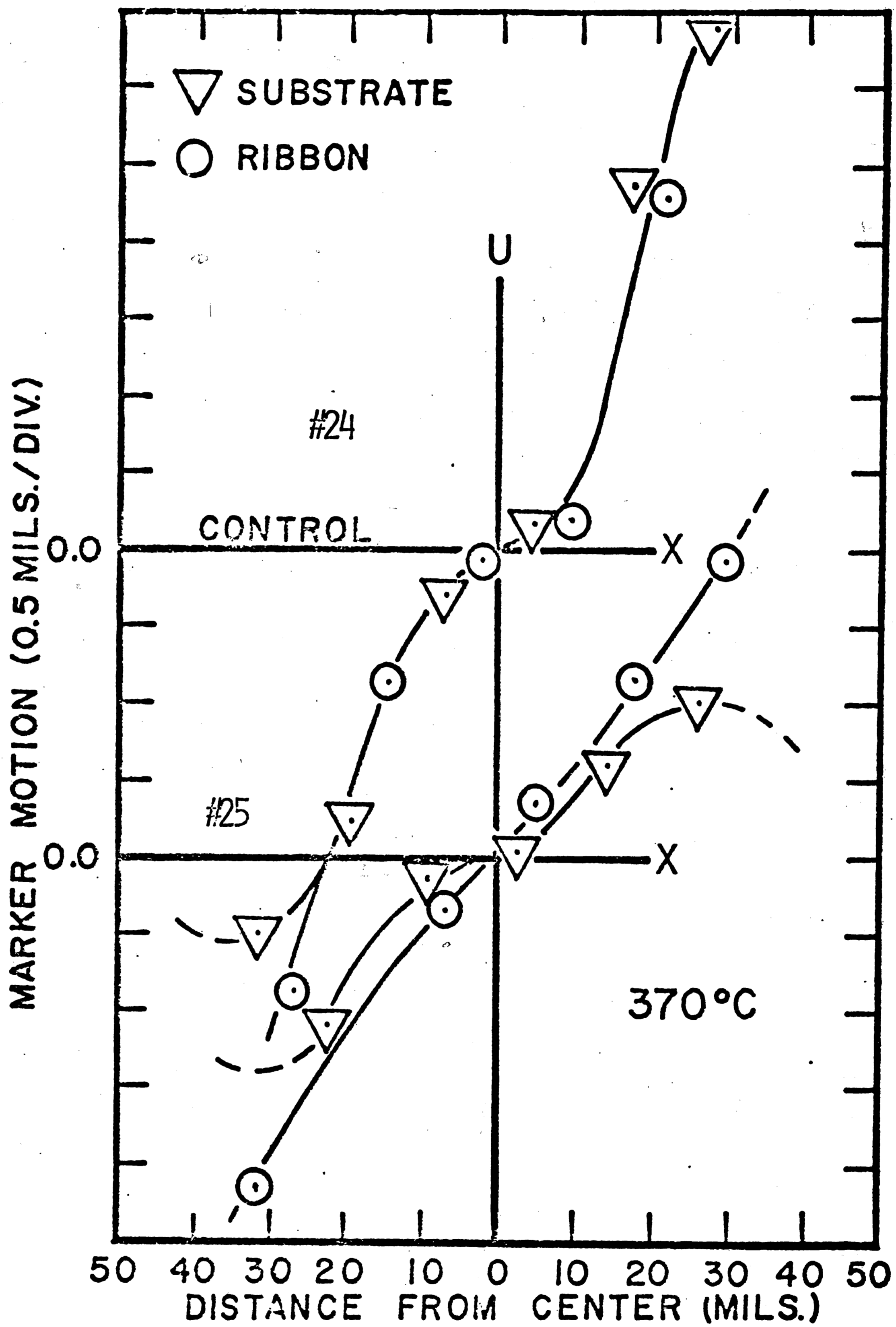


FIG. 11 MARKER MOTION VS. DISTANCE FROM CENTER FOR 370°C CONTROL AND CONTAMINATED SAMPLES.

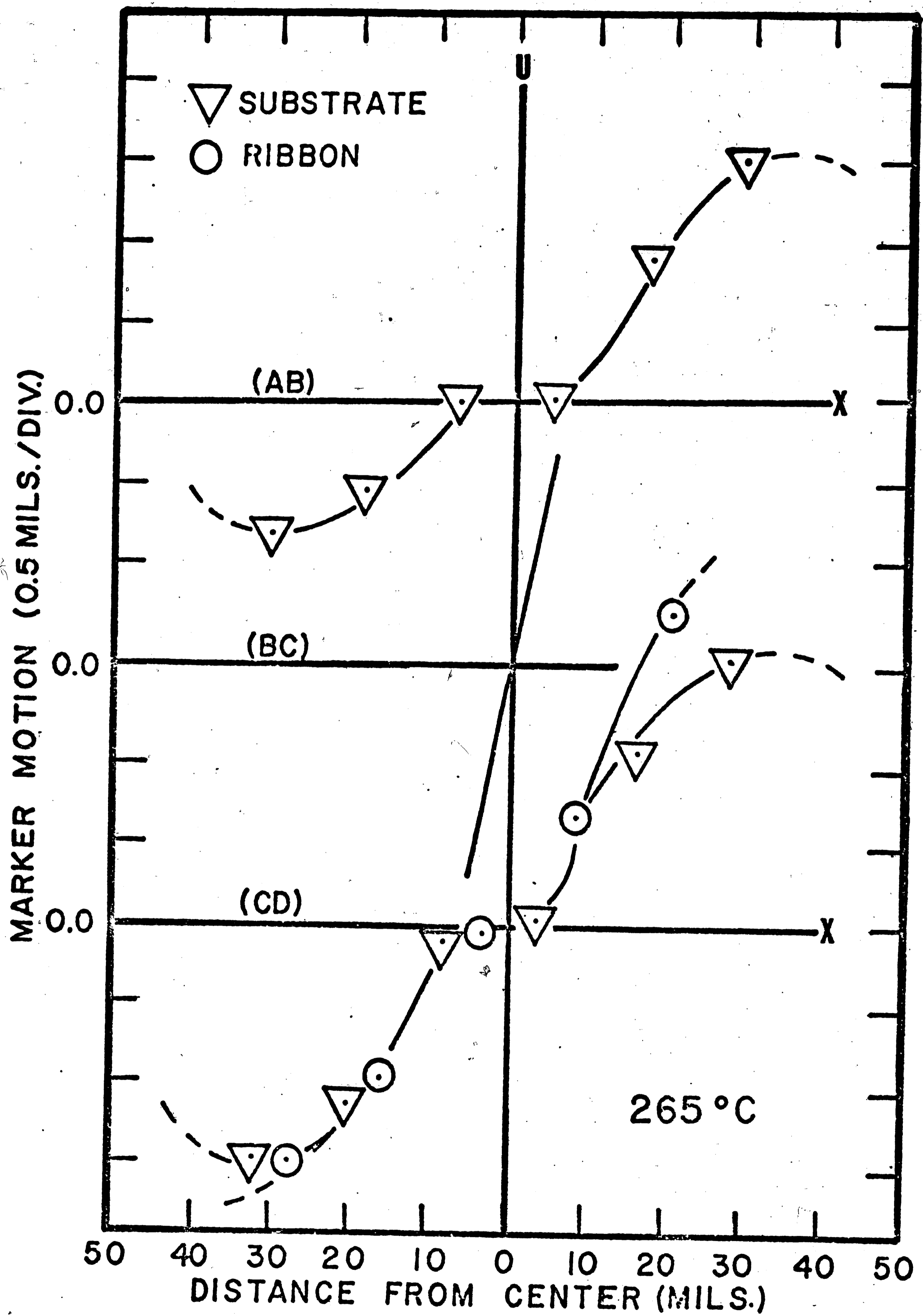


FIG. 12 MARKER MOTION VS. DISTANCE FROM CENTER FOR TWO RIBBON - TWO SUBSTRATE SYSTEM BONDED AT 265°C.

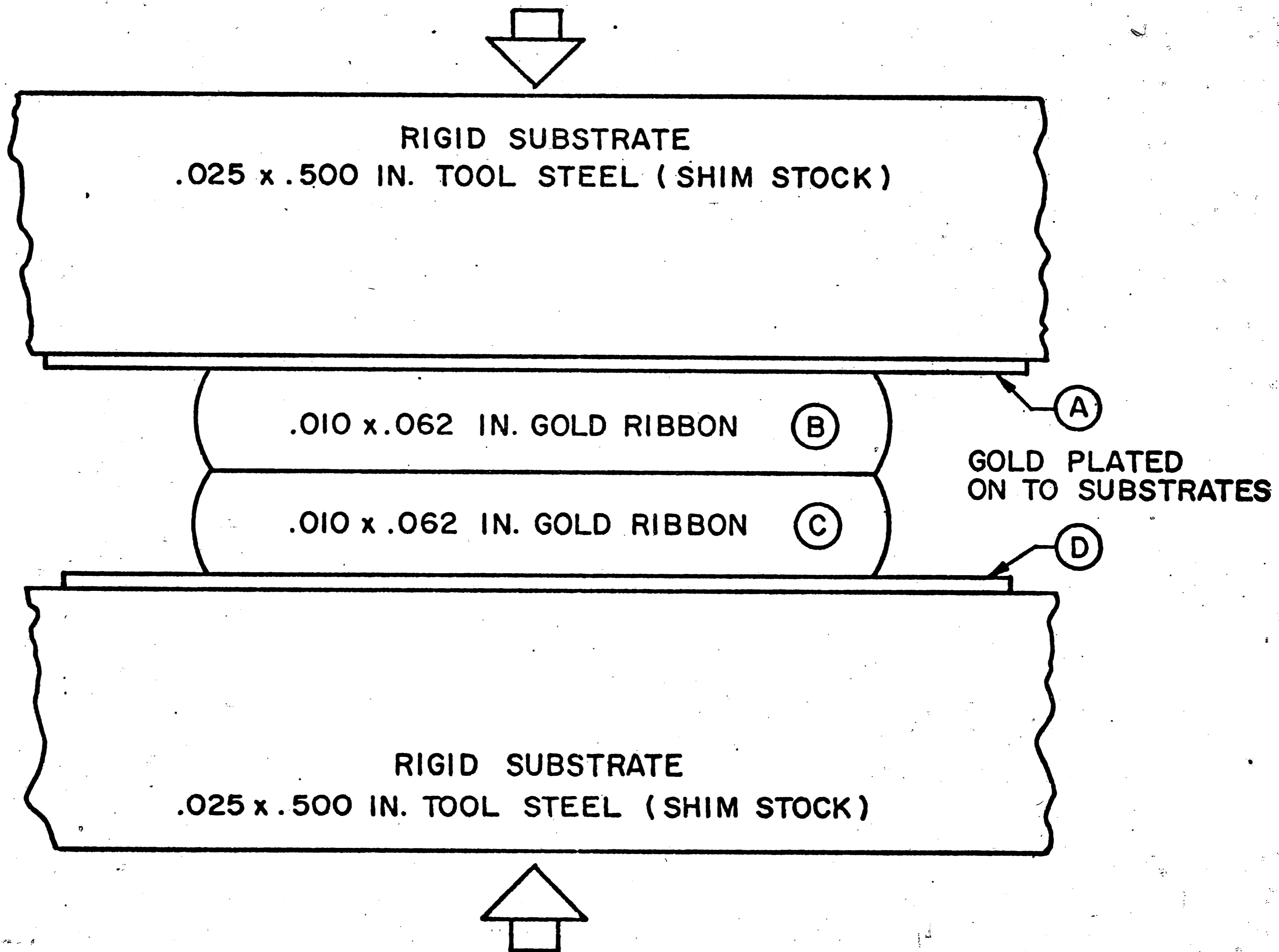


FIG. 13 SCHEMATIC ILLUSTRATION OF TWO RIBBON - TWO SUBSTRATE SYSTEM.

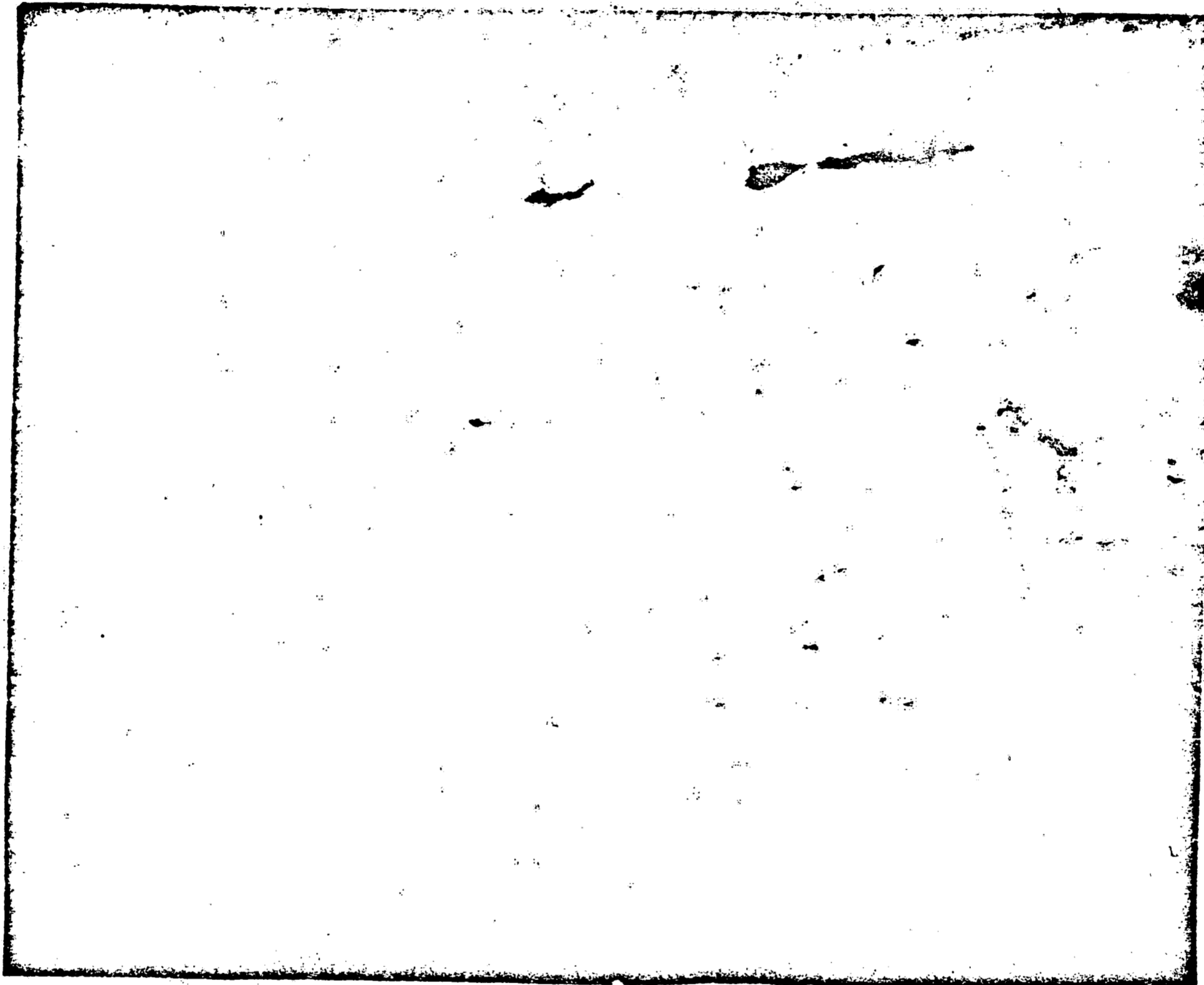


FIG. 14 SEM PHOTOGRAPH OF GOLD RIBBON SURFACE (1000X).



FIG. 15 SEM PHOTOGRAPH OF THIN SUBSTRATE METALLIZATION (400X).

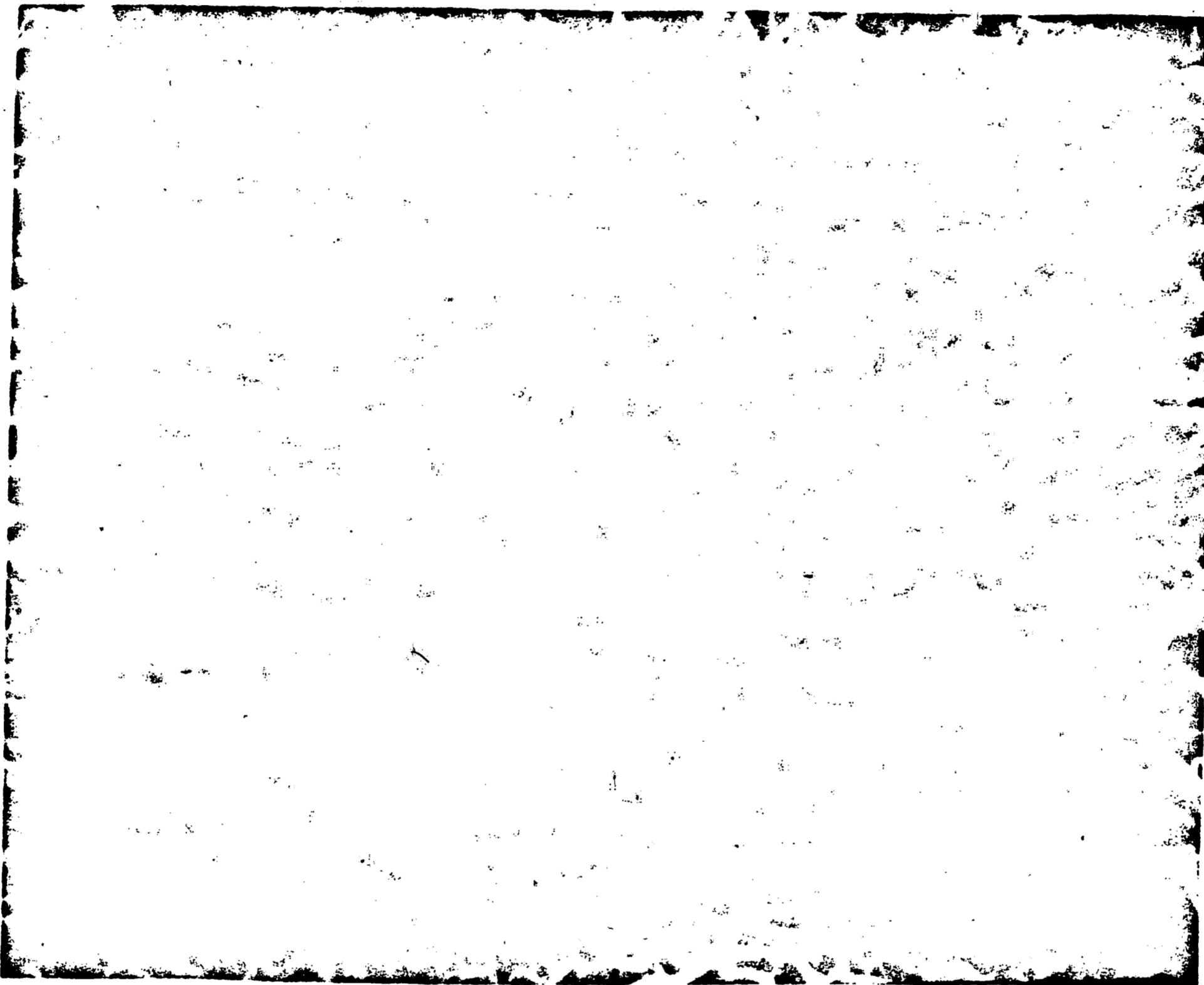


FIG. 16 SEM PHOTOGRAPH OF THIN SUBSTRATE METALLIZATION (1000X).

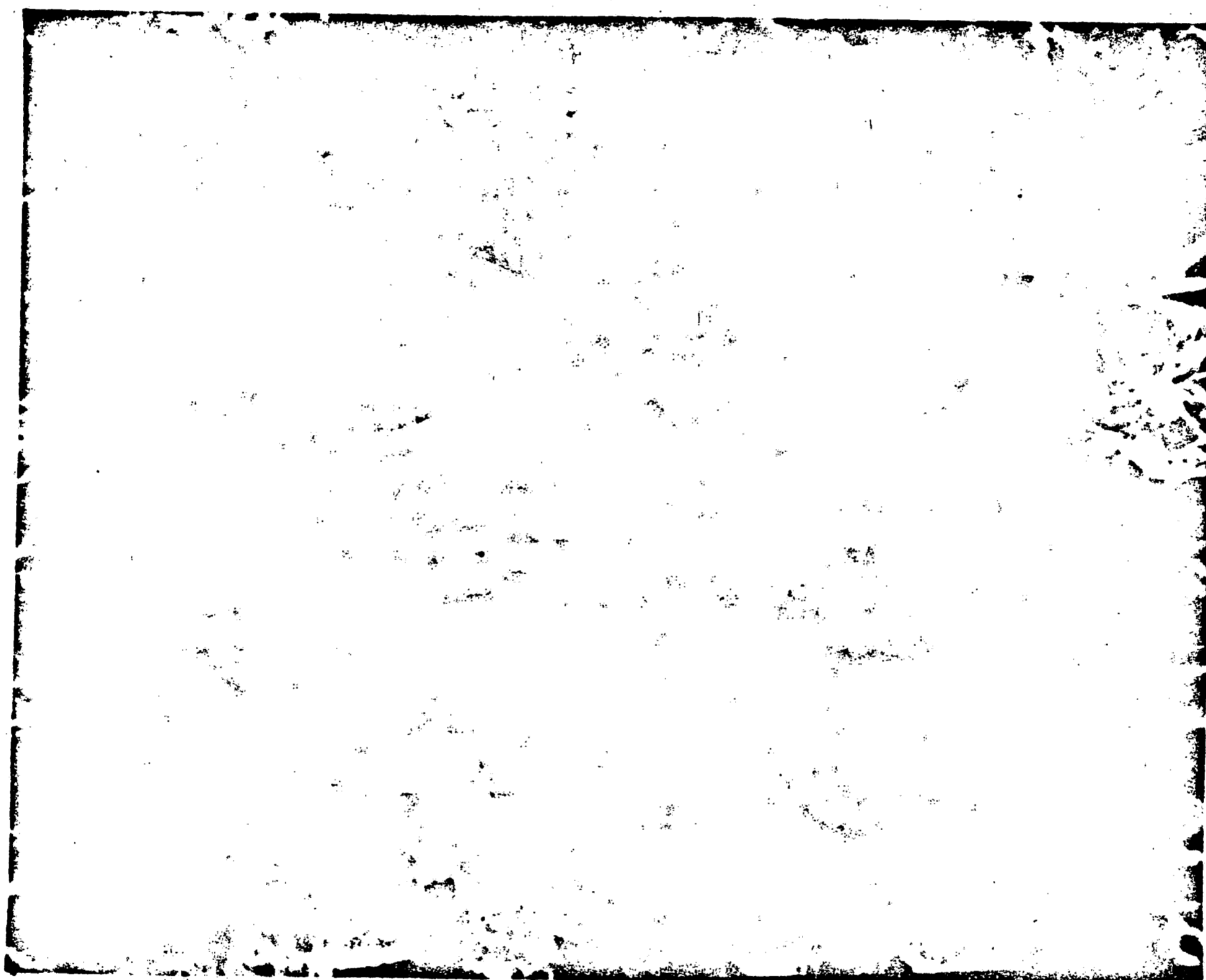


FIG. 17 SEM PHOTOGRAPH OF THICK SUBSTRATE METALLIZATION (1000X).

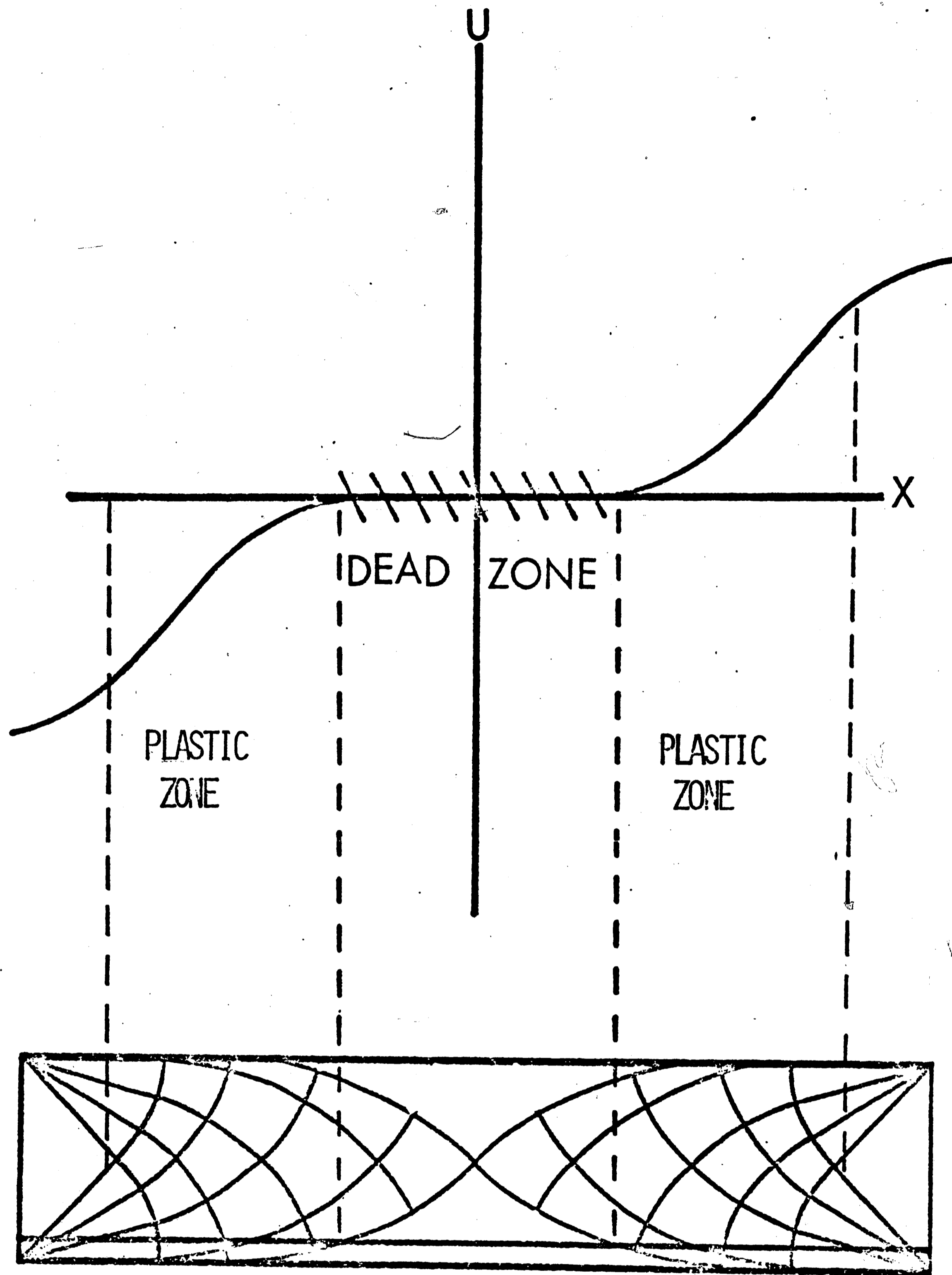


FIG. 18 SCHEMATIC ILLUSTRATION OF MARKER MOTION VS. DISTANCE FROM CENTER AS PREDICTED BY SLIP-LINE PLASTICITY THEORY.

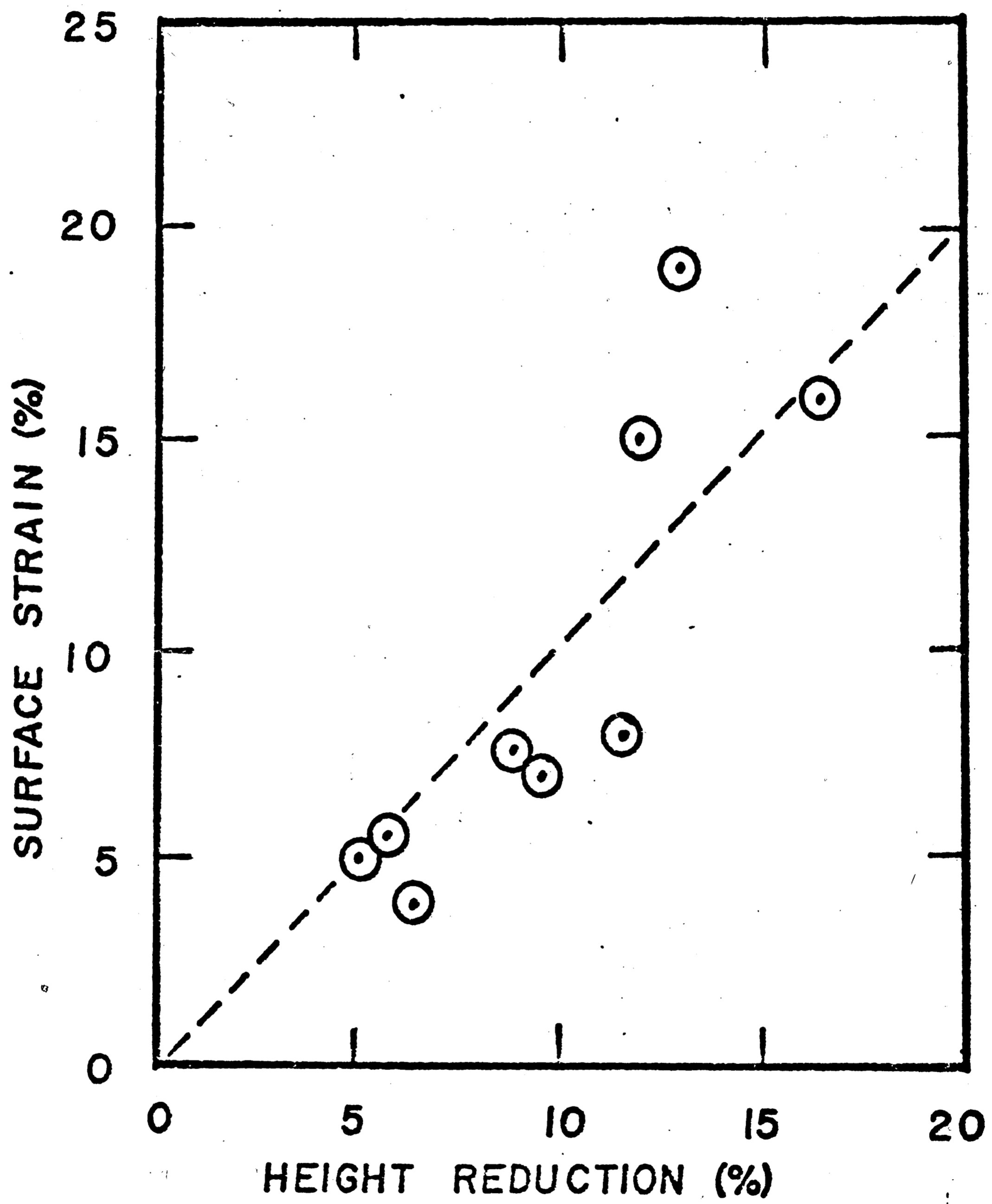


FIG. 19 SURFACE STRAIN VS. HEIGHT REDUCTION FOR THERMO-COMPRESSION BONDED SPECIMENS.

96

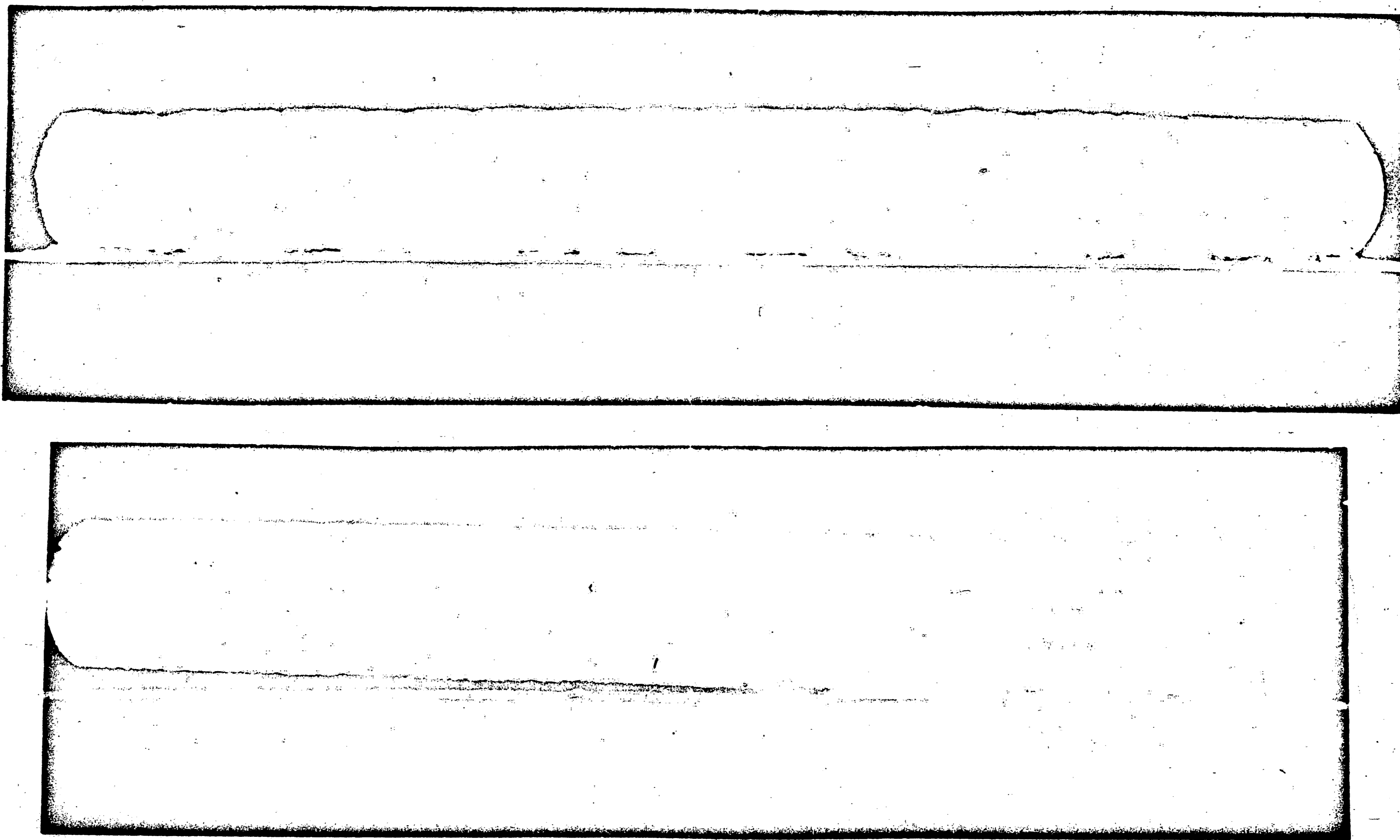


FIG.20 CONTAMINATED (LOWER) AND NON - CONTAMINATED (UPPER) SAMPLES BONDED AT 370°C.
(100X)

47



FIG. 21 PHOTOMICROGRAPH OF TWO RIBBON - TWO SUBSTRATE SYSTEM BONDED AT 265°C AND 845 LBS.

BIBLIOGRAPHY

1. Tylecote, R. F., The Solid Phase Welding of Metals, St. Martins Press, New York, 1968.
2. Milner, D. R. and Rowe, G. W., "Fundamentals of Solid Phase Welding," Metallurgical Reviews, 7, No. 12, (1962), pp. 433-480.
3. Joshi, K. C., "The Formation of Ultrasonic Bonds Between Metals," Welding Journal, 50, No. 12, December (1971), pp. 840-848.
4. Anderson, O. L., Christensen, H., and Andreatch, P., "Technique for Connecting Electrical Leads to Semiconductors," J. Applied Physics, 28, August (1957), p. 923.
5. Adams, J. R. and Bonham, H. B., "Analysis and Development of a Thermocompression Bond Schedule for Beam Lead Devices," Proceedings Electronic Components Conference, (1972), pp. 325-331.
6. Deutsch, R. J., "Assembly and Bonding of Thin Film Hybrid Circuits," Western Electric Engineer, January (1969), pp. 2-7.
7. Clark, J. E., "The Case for Beam Lead Bonding," Electronic Packaging and Production -- Microcircuit Production Supplement, October (1970).
8. Baker, D. and Bryan, I. E., "An Improved Form of Thermocompression Bond," British Journal of Applied Physics, 16, (1965), pp. 865-871.
9. Ellington, T. S., "Lead Frame Bonding," Proceedings Electronic Components Conference, (1972), pp. 357-359.
10. Christensen, H., "Electrical Contact With Thermocompression Bonds," Bell Laboratory Record, 36, (1958), pp. 127-130.
11. English, T. A. and Hokanson, J. L., "Studies of Bonding Mechanisms and Failure Modes in Thermocompression Bonds of Gold Plated Leads to Ti-Au Metallized Substrates," 9th Annual Proceedings Reliability Physics Symposium, (1971), Las Vegas, Nevada.
12. Agers, B. M. and Singer, A. R. E., "The Mechanism of Small Tool Pressure Welding," British Welding Journal, 11, (1964), pp. 313-319.
13. Martin, B. D. and Wilson, A. D., "An In-Line Laser Interferometer Applied to Ultrasonic Bonder Characterization," IEEE Ultrasonics Symposium, San Francisco, October, 1970.

14. Chen, Gordon K. C., "The Role of Micro-Slip in Ultrasonic Bonding of Microelectronic Dimensions," International Microelectronics Symposium, Washington, D. C., October 30-31, November 1, 1972.
15. Mindlin, R. D., Mason, W. P., Osmer, T. J. and Deresiewicz, H., "Effect of an Oscillating Tangential Force on the Contact Surfaces of Elastic Spheres," Proceedings 1st National Congress on Applied Mechanics, (1952), pp. 203-208.
16. Dries, Leon, "Deformation and Structural Changes Occurring at the Interface During Gold-Gold Thermocompression Bonding," Master's Thesis, Metallurgy and Materials Science, Lehigh University, Bethlehem, Pa., (1973).
17. Hill, R., Lee, E. H. and Tupper, S. J., "A Method of Numerical Analysis of Plastic Flow in Plane Strain and Its Application to the Compression of a Ductile Material Between Rough Plates," Journal of Applied Mechanics, 18, March (1951), pp. 46-52.
18. Antle, William K., "Friction Technique for Optimum Thermocompression Bonds," IEEE Transactions on Component Parts, December, 1964.

VITA

PERSONAL HISTORY

Name - Ronald Paul Stapleton

Date of Birth - August 18, 1940

Parents - Mr. & Mrs. Ted Stapleton

Hometown - Knoxville, Tennessee

FAMILY

Wife - Rita

Sons - Robert Scott and Michael Todd

EDUCATIONAL BACKGROUND

Institutions - University of Tennessee, Knoxville, Tennessee

BSEE - 1969

Lehigh University, Bethlehem, Pa.

MS Metallurgy and Materials Science

June, 1974

Honors - Eta Kappa Nu

PROFESSIONAL EXPERIENCE

1. U.S. Navy Feb., 1960 to June, 1966

2. Test Equipment Design and Development Engineer

Western Electric Company, Dallas, Texas

Jan., 1970 to June, 1972

3. Lehigh Fellowship Program

Western Electric Company, Princeton, N. J.

June, 1972 to June, 1974